NASA CONTRACTOR REPORT

NASA CR-2264

A NOVEL LASER RANGING SYSTEM FOR MEASUREMENT OF GROUND-TO-SATELLITE DISTANCES

by Kurt E. Golden, Dale E. Kind, Stanley L. Leonard, and Roy C. Ward

Prepared by
THE AEROSPACE CORPORATION
Los Angeles, Calif. 90009
for Langley Research Center

NATIONAL AERONAUTICS AND SPACE ADMINISTRATION • WASHINGTON, D. C. • JUNE 1973

1. Report No.	2. Government Accession No.	3. Recipient's Catalog No.
NASA CR-2264		

4. Title and Subtitle	5. Report Date
A NOVEL LASER RANGING SYSTEM FOR MEASUREMENT OF GROUND-TO-SATELLITE DISTANCES	June 1973
	6. Performing Organization Code

7. Author(s)	8. Performing Organization Report No.
Kurt E. Golden, Dale E. Kind, Stanley L. Leonard, and Roy C. Ward	
	10. Work Unit No.
9. Performing Organization Name and Address	
The Aerospace Corporation P. O. Box 92957 Los Angeles, Calif. 90009	11. Contract or Grant No. NAS 1-11080
	13. Type of Report and Period Covered Contractor Report
12. Sponsoring Agency Name and Address	
National Aeronautics and Space Administration Washington, D. C. 20546	14. Sponsoring Agency Code

15. Supplementary Notes

16. Abstract

A novel technique has been developed for improving the precision of laser ranging measurements of ground-to-satellite distances. The method employs a mode-locked laser transmitter and utilizes an image converter tube equipped with deflection plates in measuring the time of flight of the laser pulse to a distant retroreflector and back. Samples of the outgoing and returning light pulses are focussed on the photocathode of the image converter tube, whose deflection plates are driven by a high-voltage 120 MHz sine wave derived from a very stable oscillator. From the relative positions of the images produced at the output phosphor by the two light pulses, it is possible to make a precise determination of the fractional amount by which the time of flight exceeds some large integral multiple, N, of the period of the deflection sinusoid. The value of N is obtained with the aid of an auxiliary measurement in which the outgoing and returning light pulses are detected by photomultiplier tubes whose outputs are used to start and stop a commercial time interval meter.

A laboratory breadboard version of the system was constructed and tested on a roof-top range whose total length (down and back) was about 80 meters. The statistical spread in the results obtained with the laser ranging system corresponded to an uncertainty (standard deviation) of about 1.3 cm in the measurement of this total length. Since the uncertainty in a one-way range measurement would be half as great, this result implies a ranging accuracy of 7 mm. The average value of the total length obtained by laser ranging agreed to within 1 cm (less than the joint experimental errors) with the results of measurements made by conventional means (i.e. with a steel surveying tape).

17. Key Words (Suggested by Author(s))	18. Distribution Statement
Laser Ranging Lasers Geodesy	Unclassified - Unlimited

19. Security Classif. (of this report)	20. Security Classif. (of this page)	21. No. of Pages	22. Price*
Unclassified	Unclassified	61	$3.00

*For sale by the National Technical Information Service, Springfield, Virginia 22151

Page Intentionally Left Blank

TABLE OF CONTENTS

FIGURES

A NOVEL LASER RANGING SYSTEM FOR MEASUREMENT OF GROUND-TO-SATELLITE DISTANCES

By Kurt E. Golden, Dale E. Kind, Stanley L. Leonard
and Roy C. Ward
The Aerospace Corporation

I. SUMMARY

A novel technique has been developed for improving the precision of laser ranging measurements of ground-to-satellite distances. The method employs a mode-locked laser transmitter and utilizes an image converter tube equipped with deflection plates in measuring the time of flight of the laser pulse to a distant retroreflector and back. Samples of the outgoing and returning light pulses are focussed on the photocathode of the image converter tube, whose deflection plates are driven by a high-voltage 120 MHz sine wave derived from a very stable oscillator. From the relative positions of the images produced at the output phosphor by the two light pulses, it is possible to make a precise determination of the fractional amount by which the time of flight exceeds some large integral multiple, N, of the period of the deflection sinusoid. The value of N is obtained with the aid of an auxiliary measurement in which the outgoing and returning light pulses are detected by photomultiplier tubes whose outputs are used to start and stop a commercial time interval meter.

A laboratory breadboard version of the system was constructed and tested on a roof-top range whose total length (down and back) was about 80 meters. The statistical spread in the results obtained with the laser ranging system corresponded to an uncertainty (standard deviation) of

about ±1.3 cm in the measurement of this total length. Since the uncertainty in a one-way range measurement would be half as great, this result implies a ranging accuracy of ±7 mm. The average value of the total length obtained by laser ranging agreed to within ±1 cm (less than the joint experimental errors) with the results of measurements made by conventional means (i.e. with a steel surveying tape).

II. INTRODUCTION

Since the first artificial satellite was launched into orbit about the earth in 1957, a great deal of valuable information about the earth, its gravitational field, and its atmosphere has been obtained from careful measurements of satellite orbits and their perturbations. With the more recent development of laser ranging, the precision of measurements of ground-to-satellite distances has been sharply increased; there has been a corresponding increase in the precision of the resulting determinations of geophysical parameters. Accurate laser ranging measurements of the distance from the earth to retroreflectors mounted on the surface of the moon are also yielding more precise values for many of the dynamic parameters of the earth, the moon, and the earth-moon system.

Current operational laser ranging systems are capable of measuring ground-to-satellite and ground-to-moon distances with an uncertainty of 15-30 cm (corresponding to a time-of-flight uncertainty of less than 2 nsec). These systems typically employ giant-pulse ruby lasers generating pulses 15-20 nsec long and determine the pulse time-of-flight with the aid of electronic time-interval meters (each consisting basically of a stable oscillator, an accurate cycle counter, and an electronic interpolation circuit). It is expected that in the near future several of these systems will be upgraded by the introduction of laser transmitters producing shorter pulses and by improvements in the time interval meter circuitry. The goal is a measurement uncertainty of $\lesssim$10 cm.

Ground-to-satellite measurements with 10 cm accuracy will represent a very substantial improvement. Still greater precision is needed, however, if laser ranging measurements are to play a significant role, for example, in the effort to measure and study large-scale tectonic motions on the surface of the earth. The measurement of the distances from several points on the earth to a retroreflector-equipped satellite can lead, by trilateration, to a determination of the distances between the surface points, but the uncertainties of these determinations are, in

general, appreciably greater than those of the individual ground-to-satellite distance measurements. Although statistical averaging of many observations will improve the precision of the measurements of surface distances, this precision will still be limited by that achieved in the laser ranging measurements themselves. Since large-scale tectonic motions (e.g. continental drift) typically proceed at a rate of ~5 cm/year, or less, their detection and measurement by means of laser ranging will be difficult or impossible unless the range uncertainty can be reduced to the 2-5 cm level. Such an increase in precision could also lead, for example, to important increases in the accuracy of knowledge of the structure of the earth's gravitational field, of the rotation period of the earth, the distances from a station to the axis of rotation and to the equatorial plane, and the motion of the pole (Ref. 1).

The difficulties associated with decreasing laser ranging uncertainty below 5 cm are formidable, however. For one thing, it is necessary to correct the measured range for the effect of the refractive index of the atmosphere, a correction of several meters in a ground-to-satellite measurement. A calculated value for this correction can be obtained if the atmospheric pressure and temperature at the surface are known, but the uncertainty in the calculation for off-zenith angles is typically several centimeters or more. Another problem is that the laser return pulse is very weak, in practice, and its shape is usually severely distorted as a result of a combination of phenomena. These include statistical fluctuations and the effects of its encounter with a satellite retroreflector array consisting of a number of elements distributed over a finite area which is oriented at an angle to the beam path. As a result, the task of establishing the time of arrival of the centroid of the pulse (or its leading edge, or, indeed, any fiducial mark) is very difficult and uncertain.

One obvious step to take in the direction of overcoming these difficulties is to employ a mode-locked laser as the pulse transmitter. High-energy pulses less than one hundred picoseconds in duration are obtainable from ruby lasers, while Nd:glass lasers yield pulses shorter than

10 picoseconds. In order to take full advantage of the brevity of these pulses, of course, the satellites in question must be equipped with retro-reflectors which do not lengthen the pulse unduly (e.g. cats-eye reflectors). On the other hand, the shape of a picosecond pulse reflected from one of the existing arrays contains information about the orientation of the array. If the time resolution of the receiving system can be made great enough, this information (and thus perhaps information about satellite attitude and center-of-mass position) might be extracted from observations of the pulse shape.

The use of picosecond ranging pulses and optimum retroreflectors would still not be enough, however, to push ranging uncertainties much below 5 cm, even if the atmospheric correction problem did not exist. It is highly unlikely that any forseeable combination of sensitive light-pulse detectors with an improved electronic time-interval meter will be able to achieve the required precision. An innovation is needed if the potential advantages of mode-locked lasers are to be fully exploited.

In this report a description is given of a laser ranging apparatus incorporating a mode-locked laser and a "vernier" system which, we believe, provides the needed innovation. The novel element of the vernier system is a commercial image converter tube with deflection plates, in which the position of the deflected electron beam corresponds to the time of arrival of a light pulse at the tube's photocathode. The specific goals of the development reported here were relatively modest, a timing precision of ± 200 psec, but the potential accuracy of the method is much greater than that. A very similar method has been employed to obtain a direct measurement of the duration of mode-locked pulses from a Nd:glass laser by Bradley and coworkers (Ref. 2) and by Schelev, Richardson, and Alcock (Ref. 3). The results of these investigations indicate that it should ultimately be possible to achieve ± 5 psec accuracy in measuring the time of flight of a light pulse in a laser ranging system.

Such precise time-of-flight measurements would not lead to correspondingly precise range determinations, of course, because of the uncertainty in the atmospheric correction. Picosecond timing measurements would, however, make it possible to improve the determination of this correction by means of the so-called two-color ranging technique (Ref. 4). In this technique, the laser transmitter would provide simultaneous ranging pulses at two different wavelengths (e.g. by means of an optical frequency-doubling crystal). Measurement of the difference between the times of flight of the two pulses (as a result of atmospheric dispersion) would permit a determination of the atmospheric correction independently of any knowledge of atmospheric pressure or temperature. Even though the uncertainty in the determination of the correction is 10-30 times greater than that in the individual time-of-flight measurements, 5 psec precision would still lead to $\sim$1 cm accuracy in the atmospheric correction and thus in the overall range measurement.

The organization of the report is straightforward. Section III, which follows, is devoted to a discussion of the method of operation of the new laser ranging system and to a description of the laboratory prototype apparatus which was designed and constructed in order to permit an experimental test of the vernier concept. An account of these laboratory tests is given in Section IV, while Section V contains a discussion of the conclusions which can be drawn from these results. Finally, in Section VI, promising directions for further development are discussed.

III. SYSTEM DESIGN

A. Method of Operation.

The method of operation of the new laser ranging technique can be elucidated by referring to the block diagram of Fig. 1, which represents the laboratory prototype apparatus actually constructed. The system is made up of three basic elements: The laser source of the ranging pulse, a standard range-measurement arrangement built around a commercial time-interval meter, and a novel "vernier" in which an image-converter tube is used to increase precision by a substantial factor.

The sequence of events is initiated when the energy storage capacitor in the laser power supply is discharged through the flash lamp of the mode-locked laser. A trigger pulse is derived at that time which is delivered to the master timing control. From the train of mode-locked pulses subsequently emitted by the laser, a single pulse is selected by an electrooptic pulse selector and transmitted as the ranging pulse while the rest of the pulse train is rejected. The ranging pulse travels to a distant retroreflector and returns to the receiving optics. Samples of the transmitted and received optical pulses are diverted by beam-splitters to fast photomultiplier detectors whose electrical outputs are used to start and stop a commercial time-interval meter. The indication of the time interval meter is the basic measurement of pulse time-of-flight, and thus of range. Start and stop enable gates are provided to the time interval meter by the master timing control in order to minimize any effect of spurious pulses. These gates are provided at approximately the expected times of arrival of the start and stop pulses and are long enough to compensate for the uncertainties in the expected arrival times.

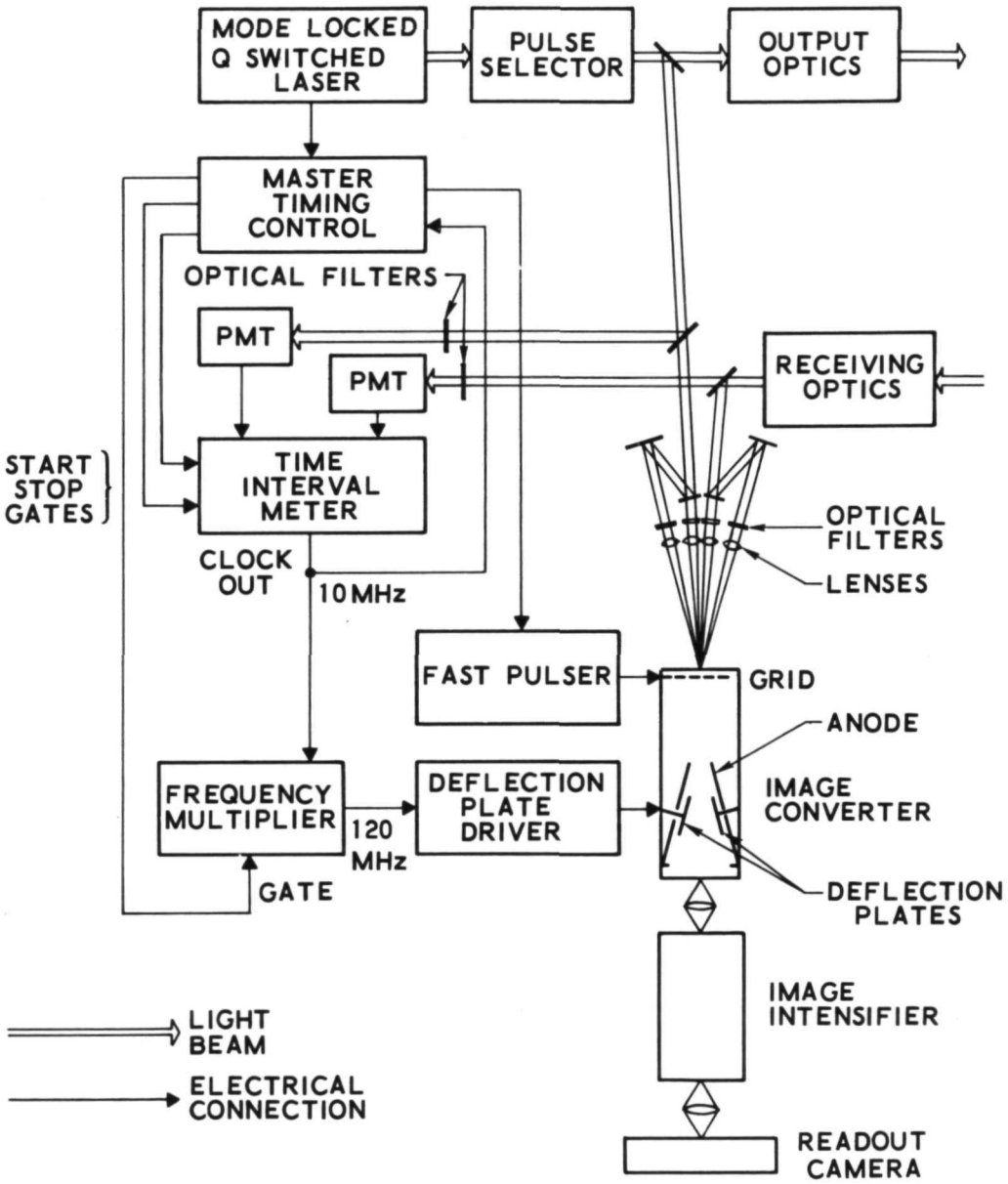

Fig. 1. Schematic Diagram of System

So far, what has been described is a conventional laser ranging system, differing from most others only in the use of a mode-locked laser. A further substantial increase in precision is provided by the vernier subsystem, in which samples of the transmitted and received light pulses are focussed on the photocathode of an image converter tube equipped with a pair of deflection plates. Each of these light pulses is further split (by an optical beam splitter) and half the energy of each pulse is optically delayed before being focussed on the image converter photocathode. These four different light beams are arranged to produce four small spots of light, one above the other, on the photocathode. The line of spots is perpendicular to the direction in which the image converter deflection plates deflect photoelectrons. Narrow-band optical filters are introduced into the light paths in order to minimize contributions from background illumination.

The arrival of each of the four pulses of light at the photocathode results in the release of a bundle of photoelectrons. These are first accelerated by a potential of about 2000 volts applied to a grid in front of the photocathode and later by a potential of $\sim$15000 volts on the anode. After being accelerated, the photoelectrons pass between the deflector plates and are deflected by a 120 MHz sinusoidal voltage derived, by frequency multiplication, from the stable 10 MHz master oscillator of the time-interval meter. At the other end of the tube, the electrons strike a phosphor screen and much of their energy is converted to optical photons. If a spot on the photocathode were illuminated steadily, the sinusoidal deflection voltage would cause the resulting beam of electrons to move back and forth across the phosphor, tracing out a straight line. A short pulse of light at a point on the photocathode produces instead a short segment of the full-deflection straight line. The segment's position is determined by the time of arrival of the originating light pulse and its length is determined by the duration of the light pulse.

Thus the arrival of the four incident pulses of light at the image converter photocathode, at four different times, results in the appearance of four differently positioned line segments on the output phosphor. The time interval between transmitted and reflected pulses is some large integral multiple, N, of the period, τ, of the 120 MHz deflection sinusoid plus an additional fraction of a period. From the relative positions of the line segments produced by the transmitted laser pulse and those produced by the reflected pulse, one can make a very precise determination of the magnitude of this additional fraction of a period. The reason for providing the two extra optically-delayed light pulses now becomes apparent. If only the undelayed transmitted and reflected pulses were used there would remain an ambiguity, since the position of a single line segment on the phosphor only indicates the instantaneous magnitude of the deflection voltage and not whether it is increasing or decreasing. If the optically-delayed pulses are also present and if the delays are properly chosen ($\sim\tau/4$ is a good choice) the ambiguity is readily resolved. The value of N can then be determined from the indication of the time interval meter, provided that the uncertainty in that indication is less than $\sim\pm\tau/2$ (or $\sim\pm4$ nsec for a 120 MHz deflection signal).

The grid in the image converter tube functions both as a control grid and as an extraction electrode. Most of the time it is supplied with a negative d c bias voltage large enough to prevent any photoelectron current from flowing in the tube. In this way the tube dark current can be kept so small that it has only negligible effect on the image produced at the phosphor. The master timing control provides a gate which activates the fast pulser circuit at the times when either the transmitted or reflected laser pulses are expected to arrive. The pulser provides a large positive gate pulse to the grid, which then permits passage of photoelectrons. This positive gate pulse is made very much larger than is required to simply remove the negative bias, however. It serves in addition as an extraction voltage, supplying the same large kinetic energy

increment to each photoelectron. The effect is to minimize the transit-time spreading (debunching) of the photoelectron bundle which would otherwise be introduced by the variations in the energies with which the electrons are emitted by the photocathode.

The image intensifier shown in Fig. 1 is needed for two reasons. For one thing, a laser ranging system intended for use over long distances must be able to respond to very weak return signals. Even when the return signal is strong, however, it must be severely attenuated before being allowed to strike the image converter photocathode. If the photoelectron bundle produced inside the tube by the incident light pulse contains too many electrons, their mutual electrostatic repulsion produces an unacceptable spreading of the image at the output phosphor. Since the actual overall light gain in commercially available image converter tubes is small, these faint input light pulses lead to output images which are much too dim to be photographed. A high-gain image intensifier is therefore included in the system, optically coupled (via a relay lens, in the laboratory breadboard) to the image converter output. The intensified image at the output phosphor of the image intensifier must then be bright enough to be photographed or detected in some other way. As indicated in Fig. 1, the laboratory prototype system utilized a conventional Polaroid film back to record the image.

The function of the deflection plate driver circuit is simply to amplify the 120 MHz signal from the frequency multiplier to the kilovolt amplitude needed in order to produce adequate deflection of the electron beam in the image converter tube. In early laboratory tests it was found that the cw power supplied to the image converter plates by the deflection-plate driver circuit was large enough to severely overheat the fine wire conductors leading to the deflection plates inside the image converter tube. It was necessary, therefore, to limit the effective duty cycle of the deflection voltage. A gate, several hundred μsec wide, from the master timing

control was used to control the output of the frequency multiplier circuit so that there was an input signal to the deflection plate driver only during the brief periods when the transmitted or reflected laser signals were expected to arrive.

As has been indicated in the preceding discussion, the function of the master timing control is to provide a variety of gate pulses to the other elements of the system. In an operational system, ranging to a moving target, logic circuitry would be used to determine the expected time of arrival of the returning ranging pulse, but in this laboratory breadboard system these expected times need only be manually adjustable. The gate delay periods are generated in the master timing control by presettable IC counters clocked (synchronously driven) by the 10 MHz reference signal from the master oscillator in the time interval meter. The operation cycle is initiated by the arrival of a trigger pulse generated by the discharge of the energy storage capacitor driving the laser flash lamp. After a manually-set delay (determined from observations of the actual time interval between this trigger and the firing of the laser) the gates for the frequency multiplier, the image converter grid, and the start-enable input of the time interval meter are generated. The durations of these gates are manually pre-set. After another manually-set delay, determined from the anticipated time-of-flight of the laser pulse, gates for the frequency multiplier, the image converter grid, and the stop-enable input of the time interval meter are generated. The timing of these gates can be adjusted so as to insure that the image converter grid pulser is at maximum voltage and the deflection sinusoid has stabilized at maximum amplitude before the arrival at the image converter photocathode of the laser pulses.

B. Apparatus Details

1. Laser and Pulse Selector

Ruby and neodymium lasers, mode-locked and Q-switched by bleachable organic dyes, have produced pulses shorter than 100 psec (Ref. 5). Such lasers have been built in several research laboratories and can be obtained from commercial suppliers, although they are not yet stock items. The ruby laser used in this project was a commercial product, designed for field, as well as laboratory, use.[1]

The heart of the laser is a ruby rod 12.2 cm long and 0.9 cm in diameter with end faces cut at Brewster's angle. It is pumped by a helical xenon-filled flashlamp, the flashlamp and most of the ruby rod being immersed in distilled, deionized water maintained close to 20°C by a heat exchanger. The laser head is midway between the two flat laser mirrors, one of which is fully reflective and the other 75 percent reflective at a wavelength of 0.69 μm. The mirrors are 114 cm apart, and the round-trip transit time of a light pulse (and thus the interval between pulses in the mode-locked train) is 8.3 nsec. The bleachable organic dye that mode-locks and Q-switches the laser is in a cell 1.5 mm thick, one face of the cell being the totally reflecting mirror. Both cryptocyanine and "DDI" dyes have been used, and both methyl alcohol and acetone have been used as solvents. The dye solution is circulated by a pump from a small reservoir maintained close to 20°C by the same heat exchanger that is used for the laser head. An adjustable-position aperture 1.5 mm in diameter, between the dye cell and the laser head, constrains the laser to oscillate in the lowest-order (TEM_{OOn}) mode in order to produce a Gaussian, axially symmetric output beam. An environmental cover, flushed with an overpressure of dry nitrogen, protects the laser components from dust and mechanical damage.

---

[1] The laser was supplied by Korad Dept., Union Carbide Corp., Santa Monica, California.

The flash lamp is pulsed by discharging an oil-filled 400 microfarad capacitor, typically charged to 4000 volts. The maximum repetition rate, established by the rate at which the capacitor is charged, is slightly more than three per minute.

The laser was the single item of apparatus which gave the most trouble in the development of the laboratory breadboard ranging system. The principal problems were produced by large and erratic shot-to-shot variations in output energy and fairly frequent failures to produce a clean mode-locked pulse train. (Two overlapping pulse trains were often observed.) Furthermore, when the assembly of the image converter system made it possible to measure the actual duration of the mode-locked pulses, they were found to be disappointingly long (> 500 psec).

In the course of efforts to improve laser reproducibility it was discovered that the weight of the environmental cover was sufficient to produce significant misalignment when it was put in place just after the laser had been carefully aligned. A method for providing compensatory torques to the mounting plate was developed, and its use resulted in substantial improvement in shot-to-shot reproducibility.

Studies were also made of the effects on laser performance of varying the nature of the dye, the nature of the solvent, the dye concentration, and the reflectivity of the output mirror. For reference purposes a standard set of conditions was selected: dye solution – cryptocyanine in methanol; dye concentration – absorption coefficient, at $\lambda = .694$ μm, $2.9\ cm^{-1}$; output mirror reflectivity – 0.75. The pulses produced under these conditions were typically 500 ± 150 psec in duration and the degree of reproducibility was at least as high as under any other set of conditions tested. Pulses produced when cryptocyanine in acetone was used were somewhat longer and less reproducible. Pulses obtained when the dye solution was "DDI" (1, 1' –diethyl–2, 2'–dicarbocyanine iodide) in methanol were significantly shorter, typically 200 psec in duration, but the reproducibility was again poorer. Mixtures of cryptocyanine and DDI gave performance intermediate between those produced by the pure dyes.

The shorter pulses produced by DDI produced substantially more pit damage to the output mirror and other optical surfaces than did those produced by cryptocyanine. Under standard conditions (i.e. cryptocyanine in methanol), the output mirror, with its high-quality "hard" coating, successfully withstood several thousand laser shots without pitting or significant performance degradation. One output mirror showed pit damage after several hundred shots when DDI was used, and similar damage was also caused to the antireflection-coated surface on the front face of the dye cell.

The pulse selector, also a commercial item,[1] is basically a Pockels cell containing a potassium dideuterium phosphate crystal placed between two crossed Glan prisms. When no voltage is applied to the Pockels cell, light polarized by the first Glan prism is deflected by the second Glan prism through a window to a high-pressure spark gap (10 kg/cm^2, 75 percent argon, 25 percent nitrogen) to which is applied a steady voltage, typically 20,000 volts, equal to about 90 percent of the self-breakdown voltage of the gap. A laser pulse of suitable intensity breaks down the gap and permits a high-voltage pulse from a charged transmission line to be applied for a time of about 8 nsec to the Pockels cell, the time delay between gap breakdown and application of the pulse being adjusted to a value of about 25 nsec by use of a cable of suitable length. During the interval when the voltage is applied to the Pockels cell, it rotates the plane of polarization of light passing through it, ideally by 90 degrees, so that the light pulse passes undeflected through the second Glan prism and can be used as the ranging pulse.

During early testing of the auxillary ranging system, it was found that radiation from the gap-breakdown current surge affected the operation of a nearby oscilloscope used in preliminary testing and that line-conducted interference caused false triggering of the time interval

---

[1] Obtained from Apollo Lasers, Inc., Culver City, California

meter. The pulse selector was therefore repackaged to minimize radiated interference, and a line filter was placed in the power supply lead to reduce conducted interference.

The separation between the laser mirrors is adjustable through a 3-cm range so that the interval between pulses can be set exactly equal to one cycle of the 120-MHz sweep applied to the deflection plates in the image converter. Then, if the pulse selector fails to reject unwanted pulses completely, the photoelectrons liberated by these pulses will be deflected to the same positions as those created by the desired pulse, and the precision of the measurement will not be degraded by apparent broadening of the pulse. In practice, the pulse selector rejects unwanted pulses well enough that it has not been necessary to exploit this capability.

2. Other Commercial Items

The photomultipliers used in the auxiliary system are RCA C31034 tubes,[1] chosen because of their very small transit-time spread and their extended red sensitivity.

The time interval meter is a commercial unit and includes an input circuit which ensures that the effective starting and stopping of the meter occur when the start and stop pulses reach exactly half their maximum amplitude.[2] According to the manufacturer's specifications, the uncertainty in a time interval measurement should be no more than ±1 nsec, if the start and stop pulses have the same rise time. Even though separate photomultipliers are used for the start and stop signals, the observed overall uncertainty in the auxiliary measurement has been less than ±2 nsec, appreciably better than is required.

---

[1] RCA Tube Div., Lancaster, Pa.

[2] Nanofast Model 536 (with M/2 Half-max Plug-in), Nanofast, Inc. Chicago, Ill.

The image converter tube is an RCA C73435U[1] unit, with modified S20 photocathode (for optimum sensitivity at the ruby laser wavelength). This readily-available commercial tube is the same as that used by the Ottawa group (Ref. 3) in their direct measurements of the duration of picosecond pulses.

The image intensifier, chosen because of its high gain and small dark current, is an EMI 9694 tube.[2] It is a three-stage device and is magnetically focussed by means of a water-cooled solenoid. The maximum light gain is in excess of 10^6. In order to minimize dark current, the version of the tube which has a bialkali photocathode was selected. This photocathode provides a good match to the P11 output phosphor of the image converter tube. The lenses used to couple the image converter to the image intensifier and the intensifier to a camera film back are rated at f/1.3 and have 80 mm focal length.[3] They are corrected especially for imaging at a magnification of 0.5.

3. Master Timing Control

The master timing control consists of the start-stop enable gate generators for the time interval meter and the mode control circuitry for the image converter. The mode control supplies the enable gates to the ×12 multiplier, which drives the deflection amplifier, and the grid of the image converter. The function is to enable the time interval meter and the image converter at the expected time of arrival of the laser pulse at the photomultiplier detectors and the image converter, respectively. These enable signals are generated after manually preset delay periods initiated by the discharge of the energy storage capacitors in the laser power supply. The delay period from the capacitor discharge to the laser light pulse output is typically 800 μseconds.

---

[1] RCA Tube Div., Lancaster, Pa.

[2] Gencom Div., Emitronics, Mc., Plainview, N. Y.

[3] CRT Paragon, Itex Optical Co., Rochester, N. Y.

The circuit for generating the delayed gates is shown schematically in Fig. 2. In normal short-range operation, both outputs are low prior to the receipt of the initiating trigger. The time interval meter is disabled and, via the mode control logic, the image converter is biased off and no sweep signal is delivered to the deflection amplifier. A positive-going step at the START TRIGGER INPUT sets latch B3, which in turn enables the JK flip-flop B2. The Q output of B2 goes high at the next positive transition of the 10 MHz clock and enables the four programable decade counters, A1, A2, A3, and A4. The counter then divides the clock by the number set in the 9's complement thumbwheel switches. When the count is reached, an output pulse a) triggers a single-shot multivibrator (D2), which generates the START ENABLE GATE OUTPUT signal, and b) resets the input latch, control flip-flop, and the counters. The delay period is thus presettable from 0.1 μseconds to 1000 μseconds in 0.1 μsecond increments. The duration of the gate signal is determined by the period of the single-shot multivibrator, D2, and is adjusted to encompass the jitter in the firing of the laser. A trigger signal is also derived from counter A4 which occurs 100 μseconds before the START ENABLE GATE and is used in the mode control logic circuit to permit enabling the image converter gate and deflection signal in advance of the arrival of the laser pulse.

The stop enable gate output delay circuit, using counters C1, C2, C3, and C4, is identical to the start enable delay circuit. It is triggered by the start enable output, and can be programmed to provide the stop enable gate signal at the expected time of arrival of the laser return pulse.

The 10 MHz clock is obtained from the master timing oscillator in the time interval meter. Its sine-wave waveshape is converted to a square-wave by the cascaded invertors B1.

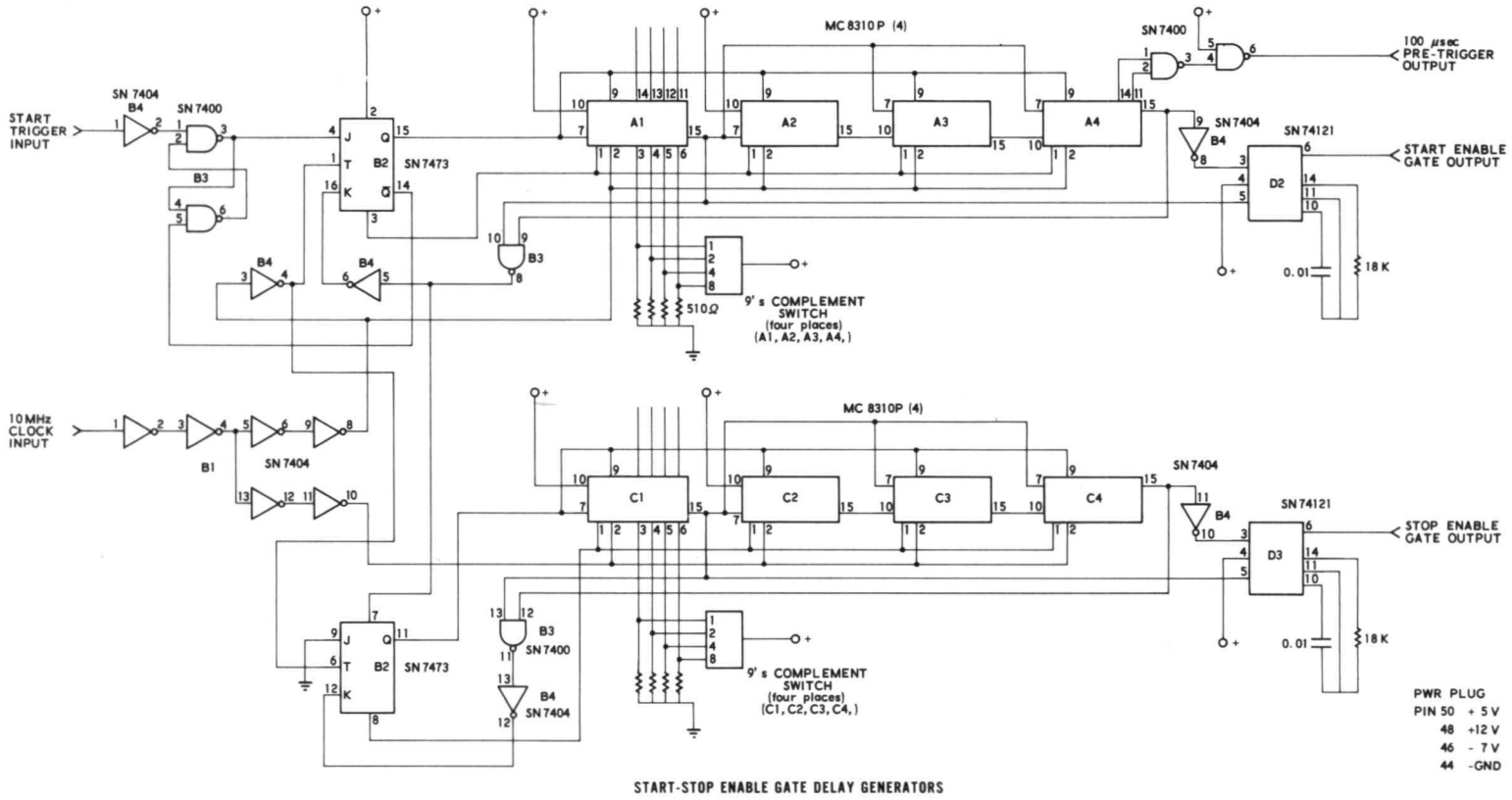

Fig. 2. Schematic of Start-Stop Enable Gate Delay Generator

The mode control circuit (Fig. 3) accepts the 100 μsecond pre-trigger and stop enable outputs from the enable gate delay generator, and an internally generated 100 pps test repetition rate (TRR) trigger. The outputs are gate control signals to the image converter grid gating amplifier and to the ×12 multiplier. The control functions are selected by three push button switches; OFF, SHORT RANGE OPERATE, TEST REP. RATE. The period of the gate control signals is determined by the period generator consisting of the μA 710 level detector, the associated RC timing network, and the discrete discharge and recharge switching transistors. In the TEST REP. RATE mode, the gate period generator is triggered by the TRR unijunction oscillator, and the gate period is self-terminated and adjustable by the period-set potentiometer. In the SHORT RANGE OPERATE mode, the gate period generator is triggered by the 100 μsecond pre-trigger. The gate period is either self-terminated or terminated by the trailing edge of the stop enable signal, whichever comes first. This feature is not necessarily used in the lab test set up, but would be utilized if testing were done at ranges long enough to require double pulsing of the image converter gates. The long range logic is not wired in, but can be accommodated through the OFF switch section.

4. Image Converter Circuits

The apparatus which provides the sinusoidal drive to the image converter plates is comprised of several parts. Mounted on the same chassis as the master timing control is a ×12 frequency multiplier followed by a filter amplifier. These circuits are driven by the 10 MHz clock signal from the time interval meter. The output is a 120 MHz voltage of sufficient amplitude to drive the high-power deflection amplifier which is incorporated into the vernier timing chassis. Also on the vernier chassis is the circuit which provides a fast high-voltage gate and extraction voltage to the image converter grid.

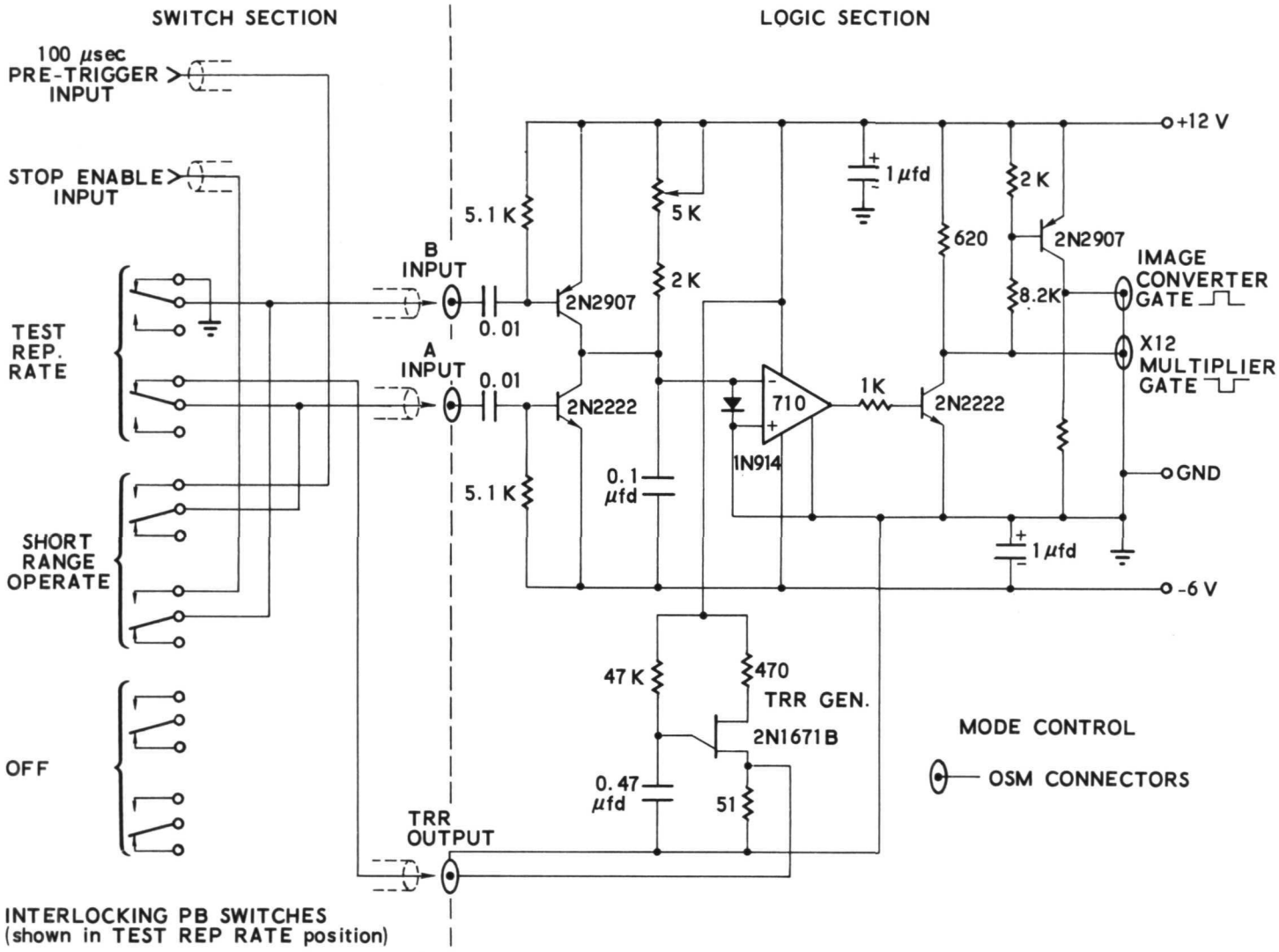

Fig. 3. Schematic of Mode Control

The gated ×12 multiplier (Fig. 4) consists of a MC1509G IC amplifier, a push-pull varactor quadrupler stage and a single-ended varactor tripler. The filter amplifier (Fig. 5) is a synchronously tuned triplet capable of producing 12 W at 120 MHz. The output is stabilized in ≈20 μseconds after the multiplier is gated on, and is sized for cw operation. However, the voltage amplifier in the image converter does not require the full output of the filter-amplifier, and the signal level is reduced with external 50 ohm attenuators in the coaxial interconnecting cable.

A simplified schematic diagram of the vernier timing chassis is shown in Fig. 6. (A more detailed schematic is provided in the Appendix, Fig. A1, along with a schematic, Fig. A2, of the power-distribution circuitry which provides the various dc voltages needed by the image converter circuits.) The basic elements of the unit include the 120 MHz deflection amplifier, image converter tube, image converter grid gate circuitry, 120 MHz deflection voltage monitor and miscellaneous biasing circuits. The deflection amplifier is a narrow-band Class B push-pull amplifier using two Eimac 4CX250B radial-beam power tetrodes. The inside of the image converter chassis is shown in Fig. 7. With maximum rated dc plate voltage, the amplifier is capable of driving the deflection plates at 3500 volts. For the maximum usable deflection of 2.8 inches on the output fluorescent screen and a deflection sensitivity of 1080 volts per inch, the deflection amplifier has to supply about 1500 volts of rf. Since it is desirable to operate the amplifier near saturation, the dc plate voltage is set at 800 to 1000 volts for maximum deflection operation.

The push-pull configuration was used because the RCA-C73435U image converter tube requires a balanced deflection voltage with respect to the anode. Two 500 pf 30 kV bypass capacitors are used in the tank circuit to isolate the 15 kV anode voltage from the amplifier tubes. The output tank circuit has an unloaded Q of about 120 and consists of transmission line tuning network, the image converter interelectrode capacitance, the plate bypass capacitors, and the deflection monitor voltage dividers. The interelectrode capacitance of the image converter tube,

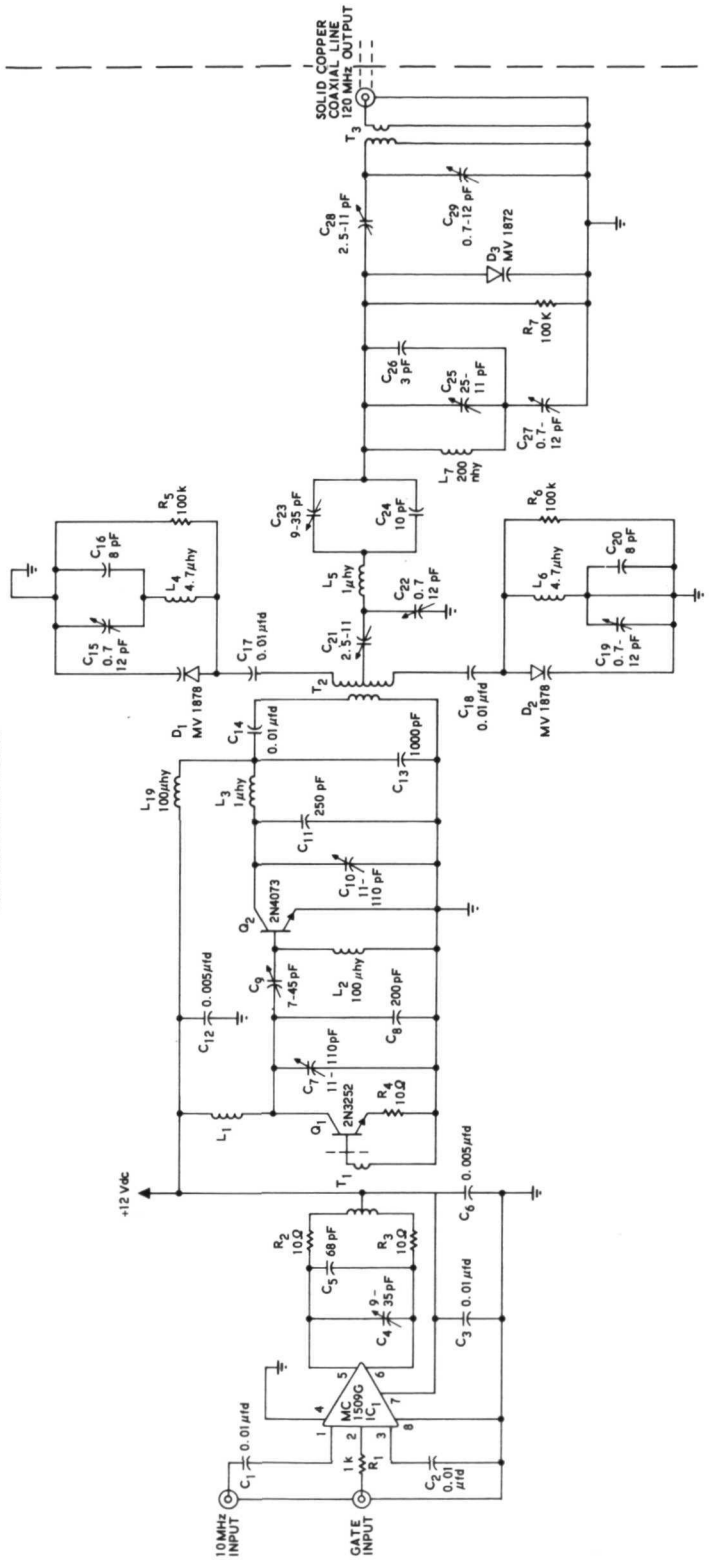

Fig. 4. Schematic of Gate and X12 Multiplier

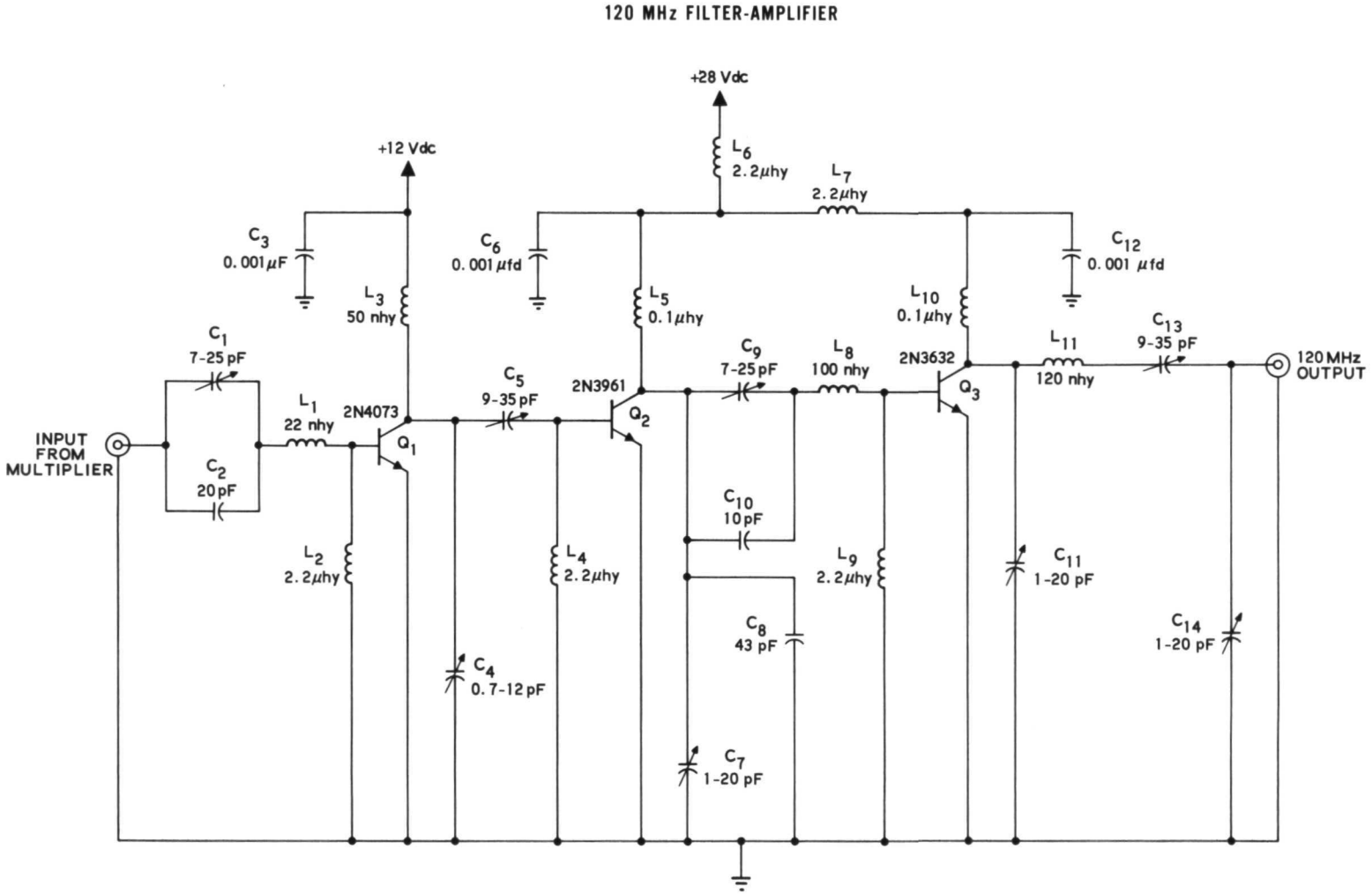

Fig. 5. Schematic of 120-MHz Filter-Amplifier

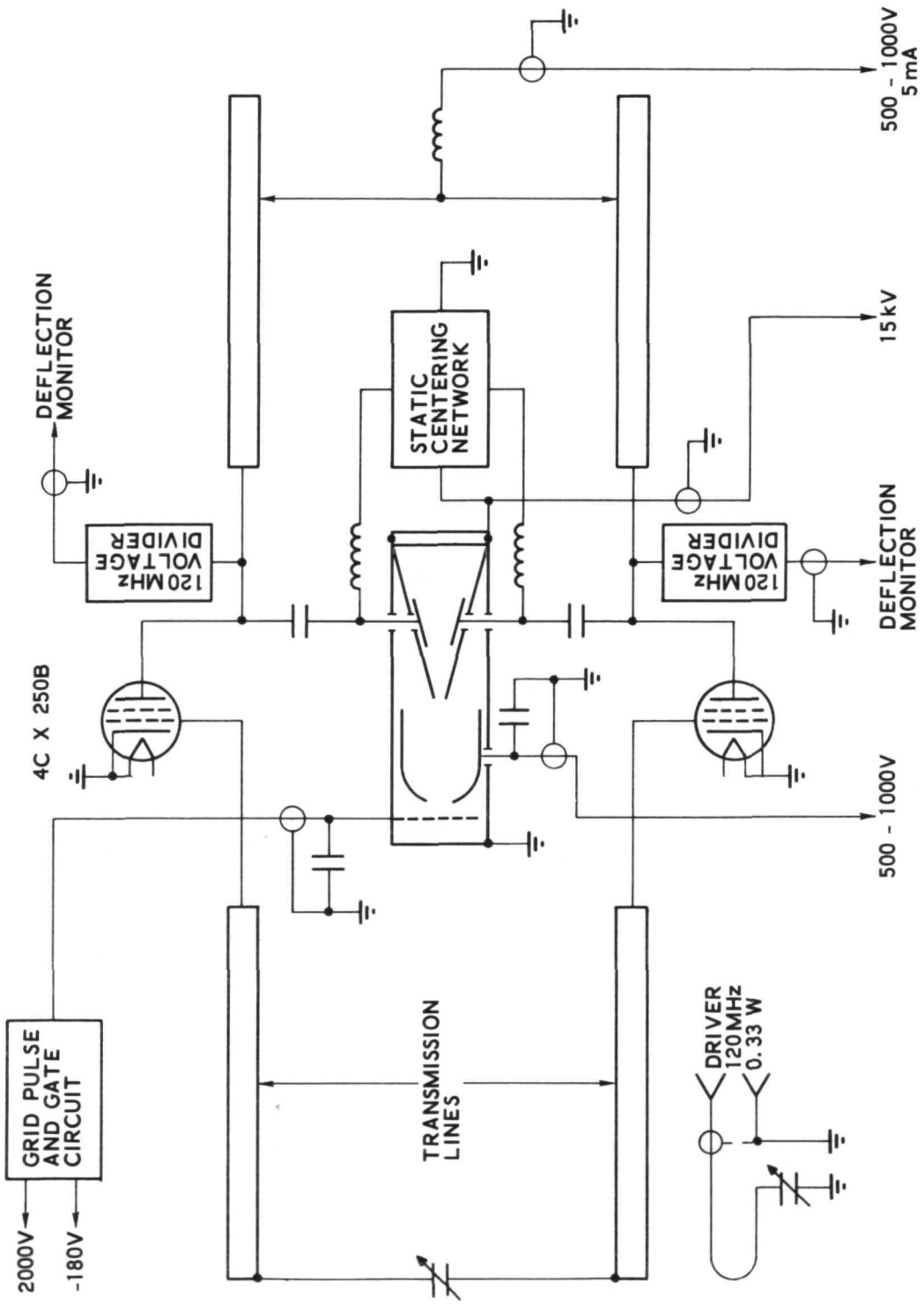

Fig. 6. Simplified Schematic of Vernier Chassis

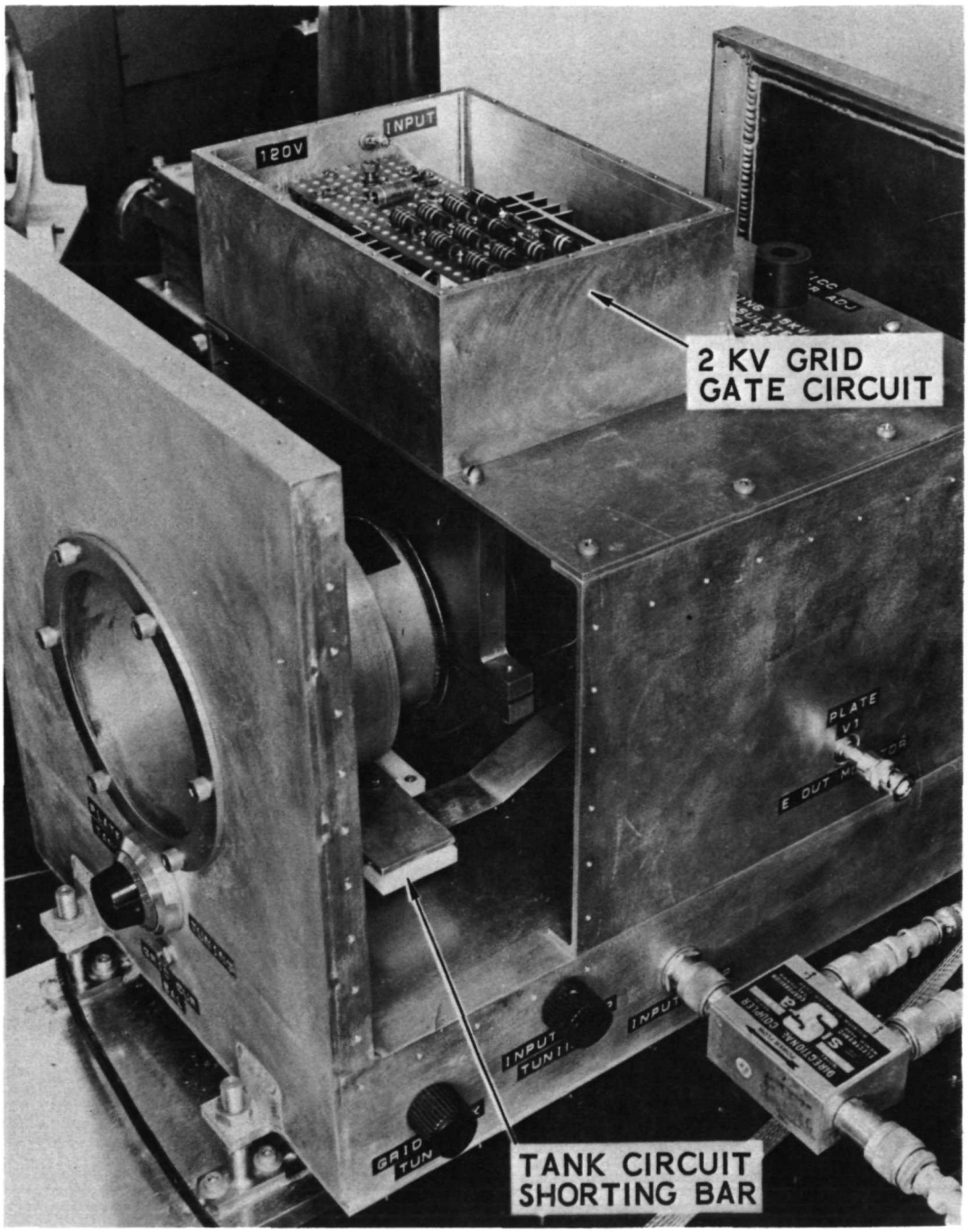

Fig. 7. Photograph of Image Converter Chassis - Side View

which effectively shunts the amplifier output, is equivalent to about 4 pf. The plate circuit is tuned by moving the sliding short shown in Fig. 7. The plate tank circuit must be tuned with the 15 kV supply on, since the capacitances of the bypass capacitors are voltage sensitive.

The input circuit consists of a coupling loop, tuning capacitors, and the resonant grid transmission line feed. The input tuning capacitors are tuned for minimum input reflections. Under the matched conditions, the power in the 120 MHz drive needed for maximum deflection is about 0.33 watts into 50 ohms. The input VSWR is less than 1.2. The underside of the image converter chassis and the grid coupling circuit are shown in Fig. 8.

The deflection monitor is a matched capacitive voltage divider. The unit was designed to reduce the output voltage by a factor of 400 and shunts each amplifier tube with about 1 pf of capacitance. At full deflection, the output monitors read 4.8 volts peak to peak. The photographs of the input and output waveforms in Fig. 9 display only the first few microseconds of the 200-300 μsec rf pulse in order to illustrate how rapidly the initial transients die out.

In order to reduce the dark-current background caused by thermionic emission, the image converter tube is cut off except during ranging measurements by a negative 180 volts on the control grid. During the actual range measurements, the grid voltage is pulsed to a positive 2000 volts for several hundred microseconds. In this mode of operation, the control grid acts as an extraction electrode, thereby minimizing transit time spreading. The negative 180 volt and positive 2000 volt grid bias voltages are supplied by a high voltage transistor switch circuit (see Fig. A1 in the Appendix). The grid pulse is triggered by the master timing control.

The input optics assembly is shown in Fig. 10 and consists of two beam splitters, two optical delay lines, four focusing lenses, four narrow-band optical filters, and a "reference spot light". When 2000 volts is applied to the control grid of the image converter tube, all photoelectrons

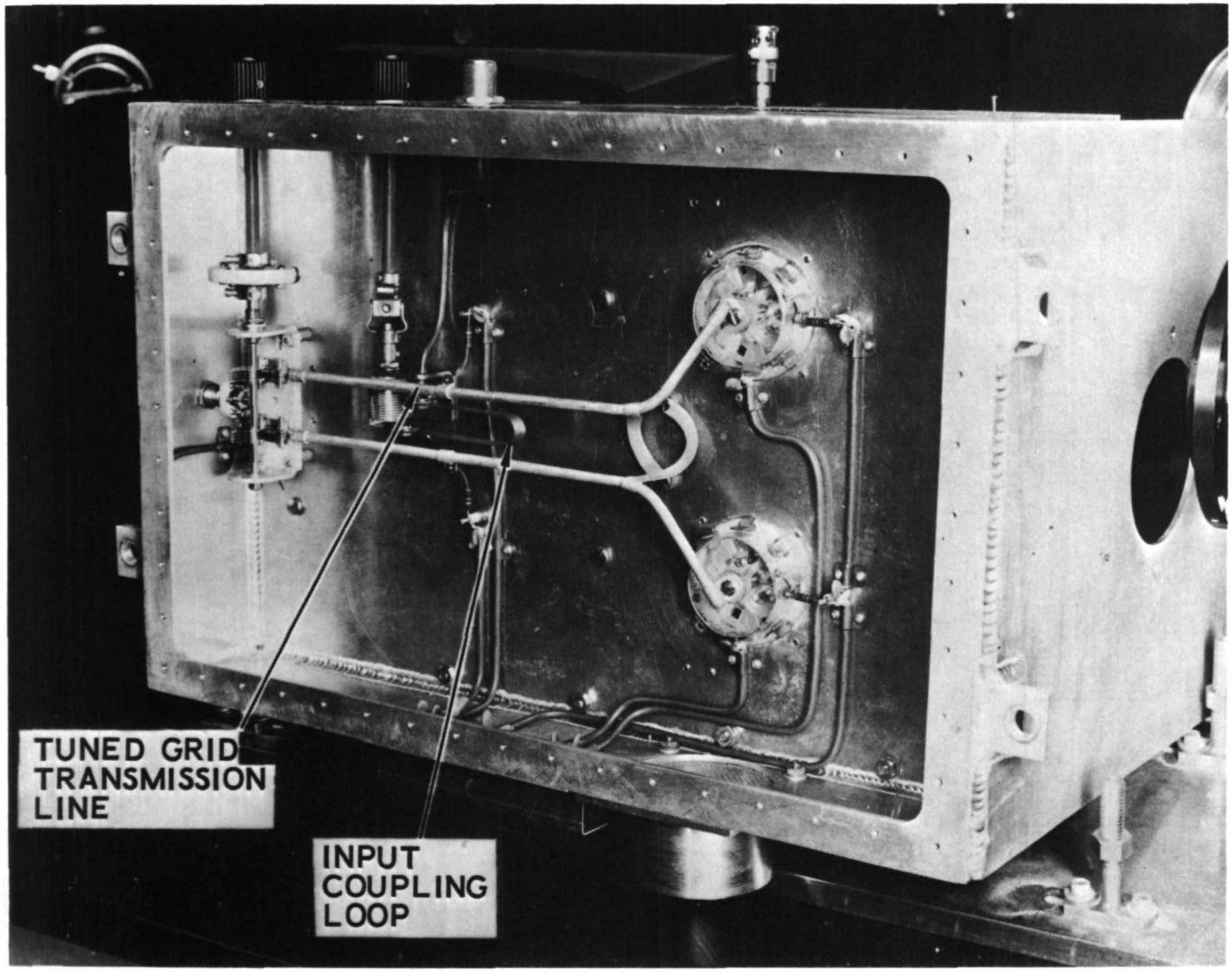

Fig. 8. Photograph of Image Converter Chassis - Bottom View

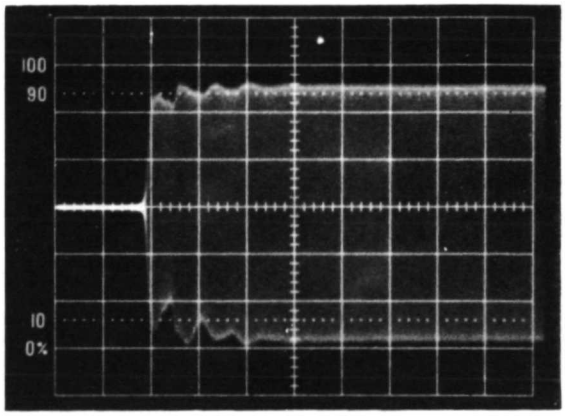

a. Input Wave-form (5 μsec/Division)
(1 V/Division)

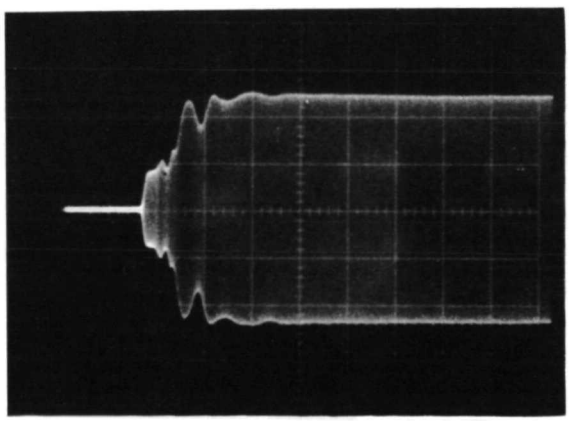

b. Output Wave-form (5 μsec/Division)
(200 mV/Division)

Fig. 9. Oscilloscope Record of Input and Output Wave-forms –
Image Converter Deflection Plate Drive

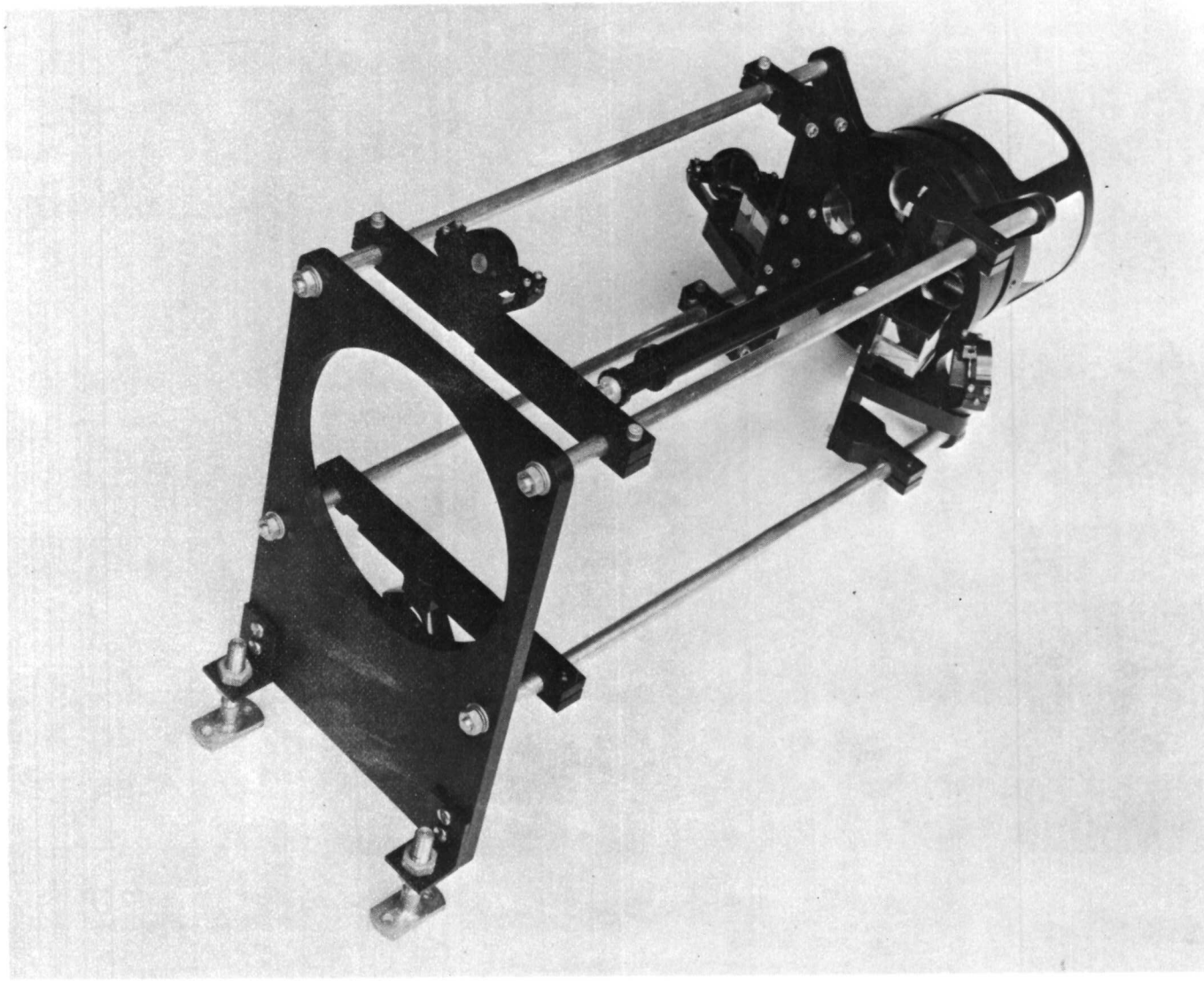

Fig. 10. Photograph of Input Optics for Image Converter

except those originating from a narrow strip on the photocathode located midway between the grid wires of the control grid (active region) are deflected off the output screen. The delay lines and reference spot light are adjusted so that all of the spots fall in line at the center of the active region. The reference spot light consists of a small tungsten-filament bulb behind a 0.025 cm circular defining aperture with a lens to focus the image of the aperture on the image converter photocathode. The line traced out on the image converter phosphor by the resulting spot serves as a reference for measuring the deflection of the laser-generated spots.

IV. TEST PROGRAM

A. Apparatus and Test Range Configuration

The only wholly convincing test of a laser-ranging concept, of course, is to employ it to measure a distance whose length can be determined independently. Accordingly, the laboratory breadboard apparatus constructed for this project was set up at one end of a roof-top range which had been established for an earlier program. The total range was short enough (~40 m each way, ~80 m round-trip) so that its length could be determined to the same, or better, accuracy with the aid of a steel measuring tape.

It may seem strange to claim any significance for the achievement of ranging accuracy equivalent to that obtainable with a measuring tape, but it should be remembered that it is not percentage accuracy but absolute accuracy which is being determined. The vernier system essentially measures the fractional amount by which the time of flight of the ranging pulse exceeds some large integral multiple, N, of the period, τ, of the image-converter deflection voltage. The accuracy with which this fraction is measured is independent of the magnitude of N. The accuracy of the auxiliary ranging system, furthermore, is sufficient to ensure that N is determined precisely, whether the range is large or small. Thus the uncertainty in the time-of-flight measurement is an absolute quantity; the measurement of a short time interval to 50 psec accuracy demonstrates the capability of measuring a much longer time interval with the same absolute accuracy. (Implicit in the above argument is the assumption that the basic 10 MHz oscillator in the time interval meter is so accurate and stable that no error arises from that source. This assumption is believed to be justified in the case of the time interval meter used in the laboratory breadboard.)

The roof-top range is shown in the photograph in Fig. 11. The laser-ranging system was housed in the structure in the left background, while the far end of the range was inside a small dome whose wall appears at the right. The laser beam travelled to the dome along the axis of one of the transite pipes visible in the photograph and returned via an adjacent pipe. In the earlier program for which the range was set up, these pipes were provided in order to minimize the effects of atmospheric turbulence. They provided the same service in this laser ranging test, of course, and, in addition, they sharply reduced the amount of stray daylight which had to be discriminated against. They also served to minimize the health hazard associated with the use of a giant-pulse laser transmitter.

In the course of the preliminary ranging tests it was found that direct sunlight on these transite pipes generated large enough temperature and density gradients in the enclosed air to produce unacceptable wandering of the laser beam. The plywood cover which is visible in the photograph (Fig. 11) was added in order to shield the pipes from vertical sunlight. For the same reason, the two central pipes (of the four available) were used for the laser beam transmission, so that horizontal protection from sunlight was also provided. These measures reduced the beam wandering to acceptable proportions.

The physical arrangement of the laser-ranging apparatus is shown in the photographs in Figs. 12 and 13. A line drawing of the optical layout (Fig. 14) is also included, both to assist in identifying the various elements of the system in the photographs and to illustrate the discussion, which follows in the next section, of the testing procedure. The layout shown in Fig. 14 is, in all essential details, identical to that shown in the diagram used in describing the method of operation of the system (Fig. 1). The only differences are that subsidiary pieces of equipment (e.g. steering mirrors) are shown explicitly, and that several auxiliary light paths are also indicated. Three of the mirrors

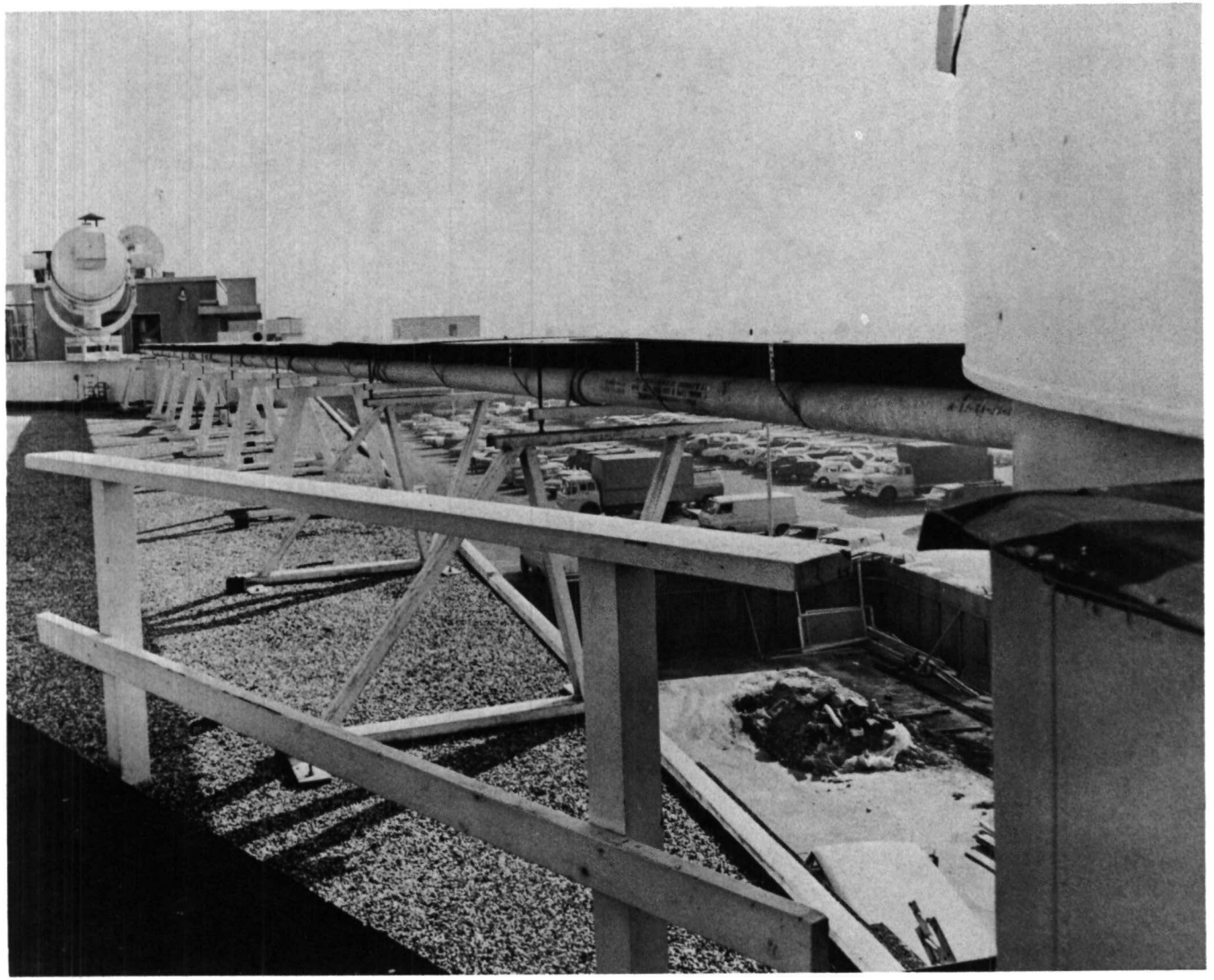

Fig. 11. Photograph of Roof-Top Range

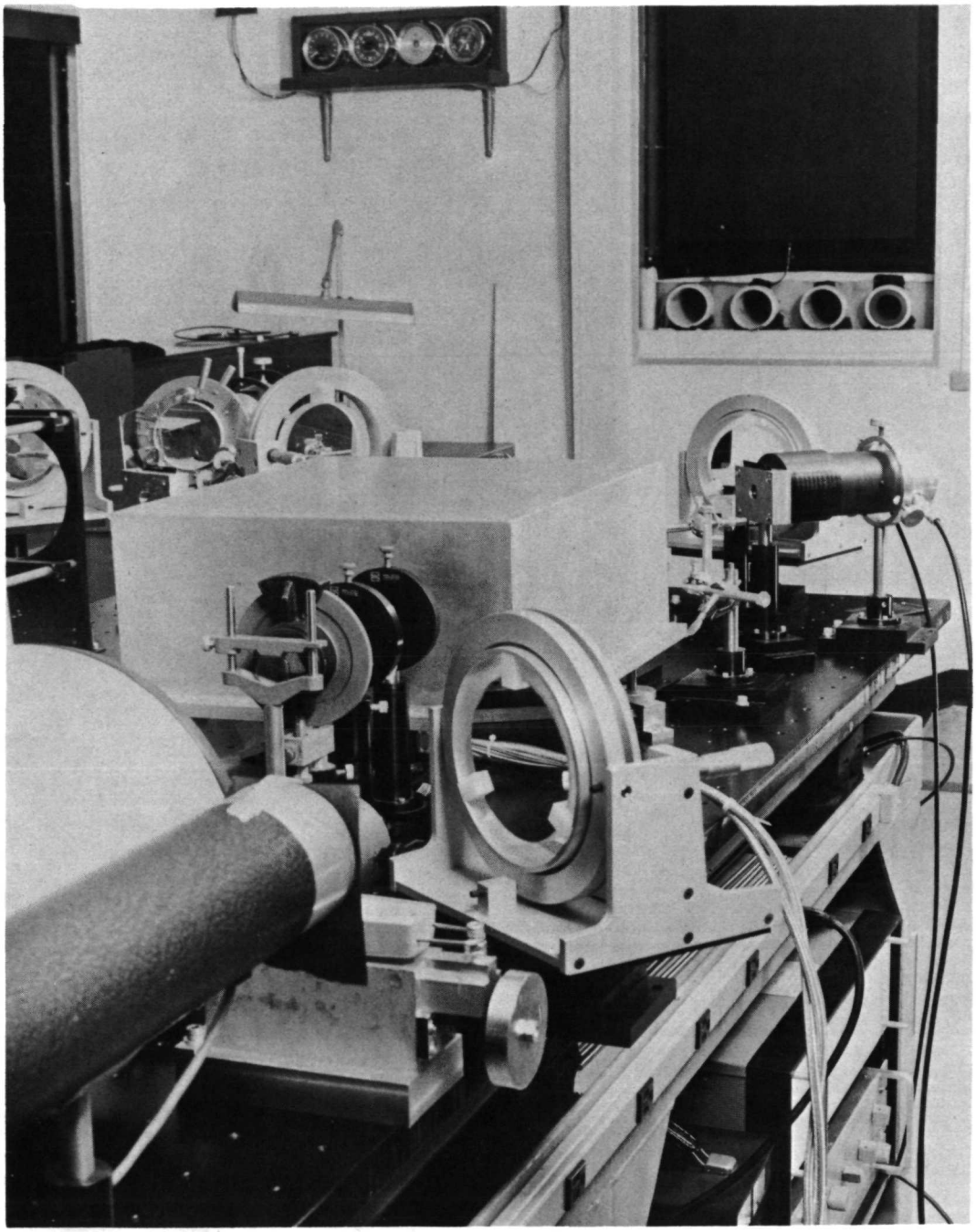

Fig. 12. Photograph of Apparatus Layout – I

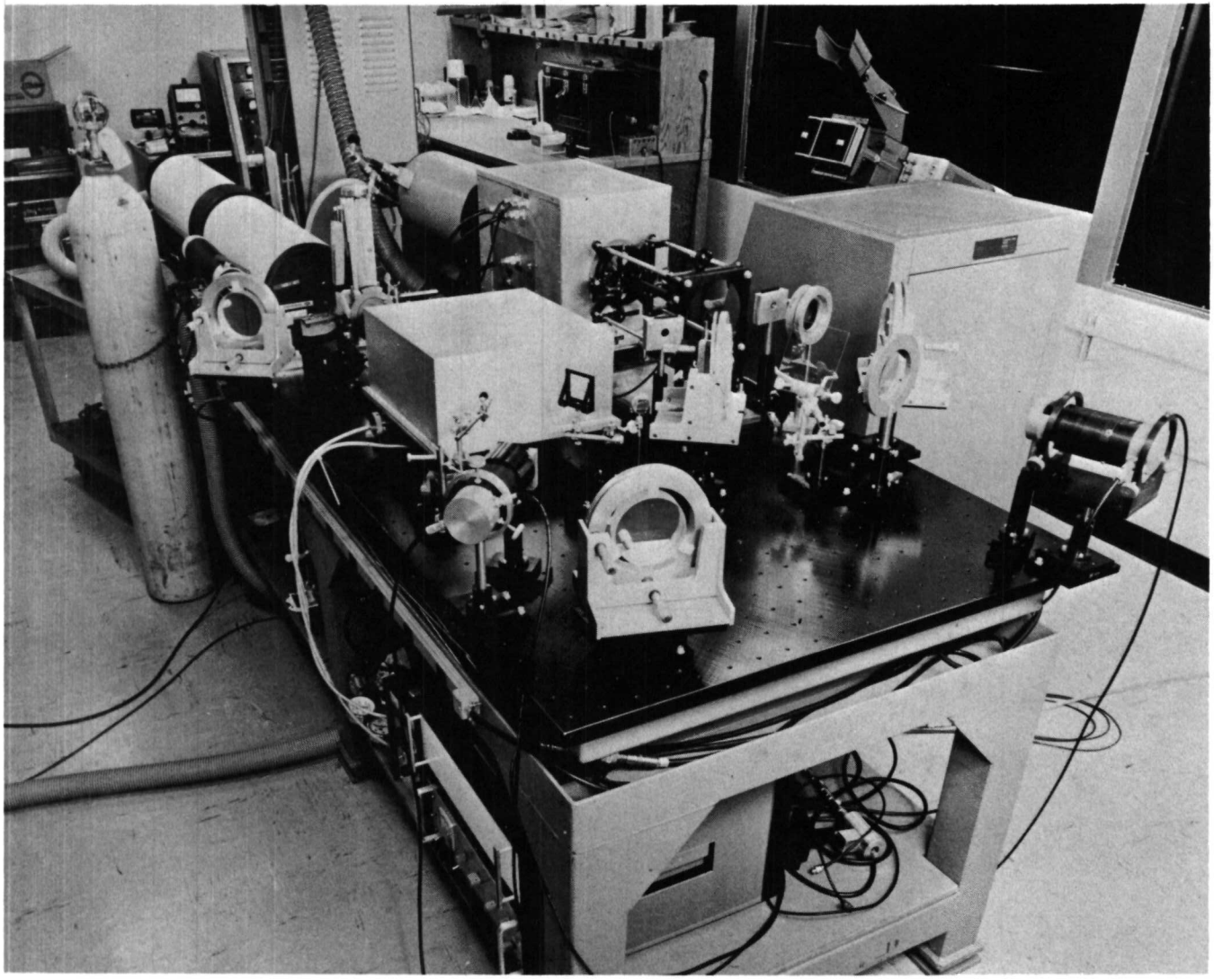

Fig. 13. Photograph of Apparatus Layout – II

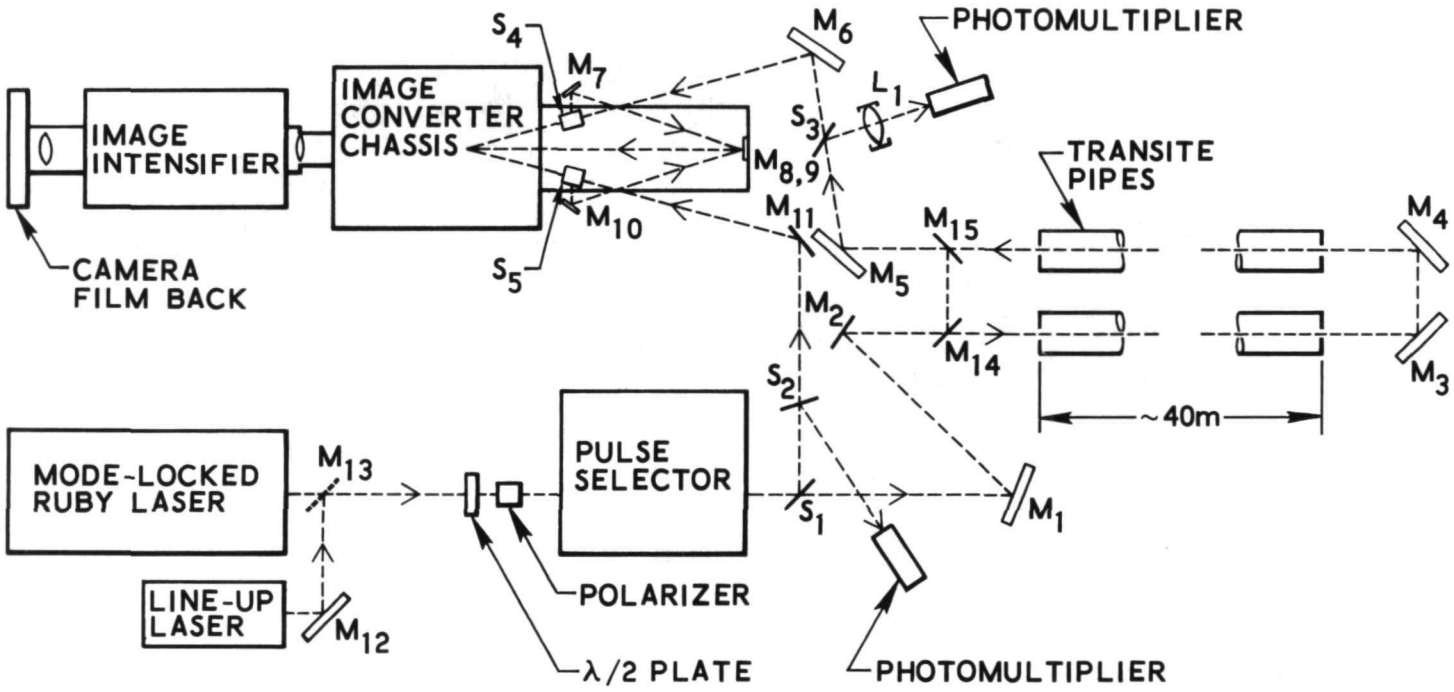

Fig. 14. Line Drawing of Optical Layout

(M_{13}, M_{14}, M_{15}) shown in the figure were not usually in the optical circuit but were introduced in order to vary the light path for testing purposes. M_{13}, in particular, was introduced when the auxiliary laser was being used to line up the optical system. Not shown in the figure is an additional beam splitter, usually placed between S_1 and S_2, which directed a sample of the outgoing pulse to a fast photodiode whose output was observed with the aid of an oscilloscope with 500 MHz band width. This photodiode was used as a monitor of laser performance.

B. Test Procedure.

After the laboratory breadboard apparatus had been assembled at the roof-top range, a number of different experimental runs were made in the course of the final shake-down phase of the development. None of these runs constituted a definitive full-scale test of the system, however. Their purpose was to expose system defects, and minor modifications and adjustments of the system were made during the test runs. In most cases, furthermore, not all of the elements of the system were functioning at the same time. Accordingly, at the close of this shake-down phase of the program, a final full-scale test was scheduled and carried out.

For the final test run, the laser dye cell was filled with a solution of cryptocyanine in methanol, with the result that the laser ranging pulses averaged 500 psec in duration. The time-interval meter was used to measure the interval between the occurrence of the trigger generated when the laser flash lamps were energized and the emission of the laser-ranging pulse (as detected by one of the two photomultipliers shown in Fig. 14). The first delay in the master timing control was set accordingly and the test sequence was begun. Since the total distance to be travelled by the light pulse was only $\sim$80 m (time-of-flight $\sim$270 nsec) the second delay was set to zero.

The first set of measurements was of the full range shown in Fig. 14. What was actually measured, of course, was the difference between the time required for a light pulse to travel over the full range (from S_1 via M_1, M_2, M_3, M_4, M_5, and M_6 to the image converter photocathode) and the time required to travel over the reference distance (from S_1 via M_{11} to the image converter). The range was then lengthened by the insertion of the additional light path shown in Fig. 15, and another set of measurements was made. Then mirrors M_{14} and M_{15} were inserted (Fig. 14) and the measurement process was again repeated for

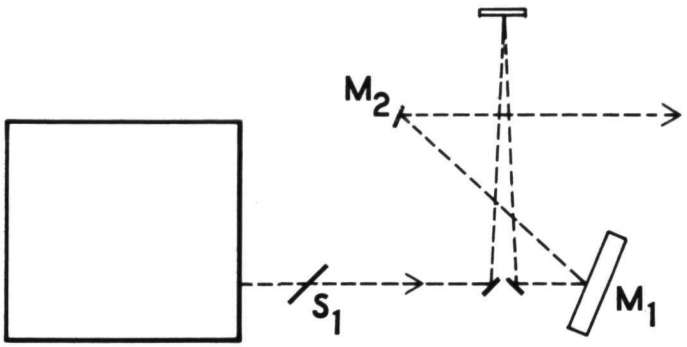

Fig. 15. Sketch of Mirror Arrangement

this "short-circuit" light path. Following the final set of laser ranging measurements, all of the light paths involved were carefully measured by conventional means, i.e. with meter sticks and steel measuring tapes. The dominant uncertainties in these measurements were those resulting from lack of knowledge of exactly where the laser beam struck each mirror. The result of each laser ranging measurement was obtained in two parts: the reading, in nsec, on the output display of the time-interval meter and a photograph on Polaroid film (Fig. 16) of the output phosphor of the image intensifier. The manner in which the range information was obtained from such a photograph is illustrated in Fig. 17. The wave-form in the upper part of the figure represents the sinusoidal deflection voltage, while the circle at the bottom encloses a schematic representation of the face of the recording phosphor. Since it was known that the time interval between direct and delayed pulses was exactly (to within experimental error) $\tau/4$, it is immediately clear that the position of the image produced by the outgoing direct pulse, for example, corresponds to point A on the deflection sinusoid rather than point B.

The distance, x, from the undeflected position to the centroid of the image produced by each light pulse was measured directly on the film record. The ratio of this distance to the half-length of the reference line was the arcsine of the phase angle of the deflection sinusoid at the time the corresponding bundle of electrons passed between the deflection plates. The magnitude of the phase angle, with respect to some arbitrarily chosen zero, could therefore be obtained with the aid of a table of trigonometric functions and a sketch like that in Fig. 17 (to assist in selecting the appropriate value from a set of angles with the same sine). The phase angles corresponding to the other light pulses, relative to the same zero, were determined in the same way, although, of course, the phase angles corresponding to the two return pulses could only be written as $2\pi N + \theta$ where N is a large (unknown) integer and θ differs from the phase of the corresponding outgoing pulse by less than 2π. The difference

Fig. 16. Photograph of Output Phosphor of Image Intensifier

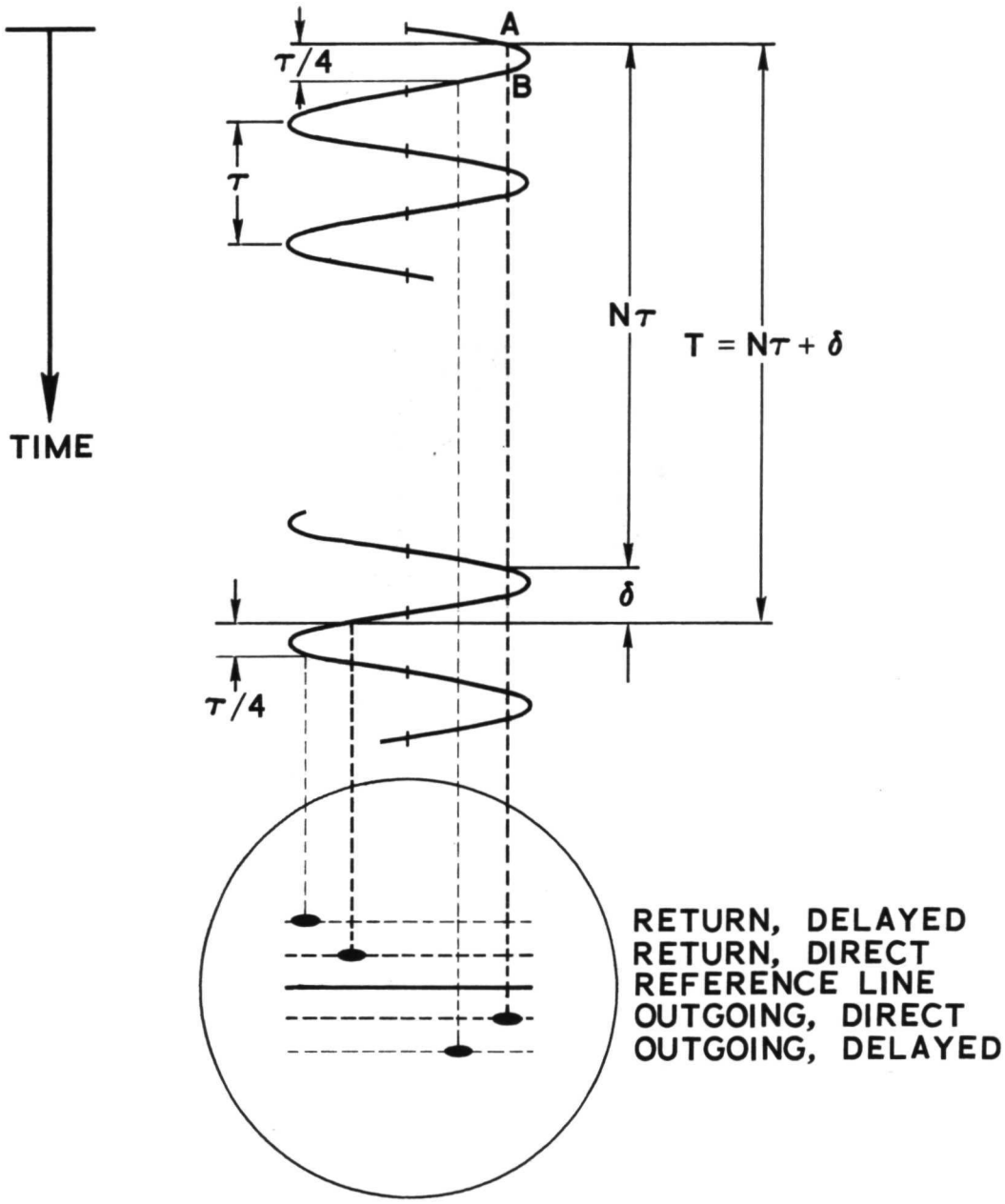

Fig. 17. Interpretation of Vernier Readout

in phase between outgoing and return pulses could then be written as $2\pi N + \Delta\theta$ where $\Delta\theta < 2\pi$. The accuracy with which the phase angle is determined is greater the nearer the corresponding image is to the center of the pattern. The values actually used in determining $\Delta\theta$ for each shot, therefore, were those corresponding to the two images nearest the center of the pattern, with addition or subtraction of $\pi/2$ as appropriate.

From the values of $\Delta\theta$ obtained in the manner described above, values of the incremental time interval δ were obtained by multiplying by $\tau/2\pi$. For each shot, therefore, the image converter record yielded a value for δ. The full time of flight being measured was thus $T = N\tau + \delta$ and the reading on the time interval meter permitted the determination of N.

The only difficulties encountered during this final test of the apparatus arose from three commercial items, the laser, the pulse selector, and the time-interval meter. The performance of the laser was somewhat less reproducible than had usually been the case when cryptocyanine in methanol was used, and substantial intensity variations were observed. More than 20% of the shots failed to produce clean mode-locked pulse trains; on most of these shots, two overlapping trains were produced. On another 25% of the shots, the laser produced a good mode-locked train, but the pulse selector passed two of the pulses in the train instead of one. (The high-voltage pulse on the pulse selector Pockels cell lasts a little longer than the interval between pulses in the train.) Since the interval between pulses in the train is almost exactly equal to the period of the deflection sinusoid, the images of two successive pulses were almost exactly superimposed at the output phosphor and little error was produced in the vernier measurement. The performance of the stop channel of the time interval meter had, however, deteriorated substantially from its original quality and produced erratic readings whenever the laser emitted overlapping trains and, usually, whenever the pulse

selector passed a two-pulse pair of which the first pulse was the smaller. Furthermore, on about 19% of the shots, the degradation of the stop channel prevented the time interval meter from registering at all, even though otherwise acceptable laser pulses were generated. This deterioration was also indicated by an appreciably larger spread in the readings for a given actual range than had been observed during the preliminary testing period, but the corresponding uncertainty in the auxiliary ranging measurement remained within acceptable limits.

As a result of the above difficulties, only 42% of the shots were completely acceptable: good clean mode-locked trains were obtained, the pulse selector selected a single pulse (or at least one large pulse followed by a very small one), and the time interval meter gave a reading. On an additional 19% of the shots, all went well except that the time interval meter gave no reading.

C. Results.

The results achieved in the final full-scale test are summarized in Table I. The laser distance values are obtained by multiplying Δt by the velocity of light (2.997925×10^{10} cm/sec) and dividing by the group index of refraction of air (1.000278). This index is, of course, a function of temperature and atmospheric pressure, but the error resulting from deviations from standard conditions, for the short 80 m distance, is no larger than about 0.1 cm. The indicated uncertainties in the laser measurements are statistical (standard deviation), while the uncertainties in the steel tape values are estimates based on the repeatability of the many separate measurements involved. In order to avoid confusion, the readings of the time-interval meter (the coarse ranging measurement) are not given in Table I. Those readings, for the three indicated distances, were 271 ± 1, 273 ± 2, and 5 ± 1 nsec, respectively. The indicated errors are again statistical variations (standard deviations) from the mean. From these readings were derived the values for N given in Table I.

Table I

Steel Tape Distance (cm)	Laser Ranging Measurements			
	δ (nsec)	N	$N\tau + \delta$ (nsec)	Distance (cm)
8098.3 ± 1	3.55 ± 0.045	32	270.22 ± 0.045	8098.9 ± 1.3
8190.4 ± 1	6.62 ± 0.041	32	273.29 ± 0.041	8190.6 ± 1.2
157.2 ± 1	5.27 ± 0.036	0	5.27 ± 0.036	158.1 ± 1.1

The agreement between the laser ranging measurements and those obtained by conventional means is seen to be very good, well within the accuracy of the separate measurements.

The results displayed in Table I were obtained, it will be recalled, when the average laser ranging pulse was 500 psec (15 cm) long. It is clear from the consistency of the data that the centroid of the light pulse can be located, nonetheless, to a precision of about 40 psec. Some earlier measurements, obtained when the laser dye cell was filled with a solution of DDI in methanol, utilized laser pulses which averaged 200 psec in length. The results are displayed in Table II. The coarse ranging system was not functioning during these shots but had been used in making several measurements of the same distance shortly before. The ranges involved were slightly different from those measured in the final test run, but they, too, were measured by conventional means just before the laser ranging measurements. Table II reveals that the overall accuracy achieved in the laser ranging measurements is no better than that obtained in the final test run in spite of the substantially shorter ranging pulses. Ability to locate the centroid is evidently not significantly improved.

Table II

Steel Tape Distance (cm)	Laser Ranging Measurements			
	δ (nsec)	N	$N\tau + \delta$ (nsec)	Distance (cm)
8168.1 ± 1	5.89 ± 0.061	32	272.56 ± 0.061	8168.8 ± 1.8
8217.1 ± 1	7.49 ± 0.042	32	274.16 ± 0.042	8216.8 ± 1.3
124.0 ± 1	4.16 ± 0.037	0	4.16 ± 0.037	124.7 ± 1.1

V. CONCLUSIONS

A design has been developed for a new type of laser ranging system employing a giant-pulse mode-locked laser transmitter and an image converter tube equipped with deflection electrodes. The image converter tube is used to make a precise measurement of the fractional amount by which the time of flight of the ranging pulse exceeds an integral multiple of the oscillation period of a very stable oscillator. An auxiliary measurement is used to determine the value of the integral multiplier.

A laboratory breadboard version of the system was constructed and tested on a roof-top range whose total length (down and back) was about 80 meters. The round-trip time of flight of the laser pulse over the 80 meter distance was measured with a statistical (rms) uncertainty of less than 45 psec (corresponding to a total distance uncertainty of less than 1.4 cm or a one-way range uncertainty of less than 0.7 cm). The total down-and-back distance deduced from the time of flight agreed to within ± 1 cm (well within the joint experimental errors) with the result of a measurement made by conventional means (i.e. with a surveying tape). Since the precision of the image converter determination is independent of the range, these results demonstrate the basic capability of the breadboard system to measure much longer times of flight to the same ~ 50 psec uncertainty.

It can therefore be concluded that a) the basic feasibility of the image converter vernier concept has been verified in practice, and b) an operational system incorporating the same commercially available components would be capable of measuring a ground-to-satellite distance with 1 cm accuracy (except for the uncertainty in the correction for the refractive index of the atmosphere) if the satellite retroreflector does not lengthen the optical pulse.

VI. FUTURE POSSIBILITIES

Adapting this novel technique for use in operational laser-ranging systems would be a quite straightforward process. If the full potential advantage of picosecond ranging pulses is to be exploited, it will also be necessary to introduce satellite retroreflectors which do not lengthen or distort the reflected pulse, e.g. cat's-eye reflectors. For routine operational use, the vernier system would have to be equipped with some sort of real-time read-out device to replace the photographic camera of the breadboard system. One obvious possibility is the use of a low-light level television tube to record the image on the image-intensifier phosphor. A camera incorporating a tube of the SIT (silicon-intensifier target) variety, for example, would have adequate sensitivity (especially if fiber optic coupling were used) to detect the light produced by a single photo-electron in the image intensifier. Tube resolution would also be adequate at this light level. The target in a SIT tube is capable of storing the exposure information for many seconds; this information could therefore be read out as a video signal at the convenience of the operator. Electronic logic circuitry (perhaps a mini-computer) would then be used to deduce the range from the video signal and the time-interval meter reading.

Interpretation of the vernier readout would be somewhat simplified if the image converter tube were equipped with two sets of deflection plates, orthogonal to each other. (Such tubes have recently become available commercially.) If the two sets of plates were driven in quadrature, the image points on the output phosphor would trace out circles rather than straight lines. The phase ambiguity would be removed and only the outgoing and return laser pulses, themselves, would need to be displayed.

It must be conceded that a vernier system consisting of an image converter tube, an image intensifier (especially a magnetically-focussed one), and a television camera tube would be cumbersome and inconvenient to use. There is no reason, however, why the whole system could not be built into a single tube (i.e. in a single evacuated envelope). The first stage of such a tube would consist, no doubt, of all the elements of an image converter tube with the exception of the phosphor screen. The screen would be replaced by a mosaic of solid state (e.g. silicon) detectors, perhaps resembling the target of a SIT tube. The information could then be read out by a scanning beam. Another possibility would be to use a charge-coupled device (Ref. 6) either as the target itself or as an auxiliary mechanism to read out information stored in a separate detector array. In such a tube the losses associated with the intermediate conversions of electrons into photons and back again would be eliminated. If further electron gain were required, one could build in a microchannel electron multiplier at an appropriate location.

In any of these versions of the vernier system improved time resolution can be obtained if the deflection frequency is increased. In the construction of the laboratory breadboard apparatus it proved easier than had been expected to provide the required high voltage on the deflection plates at 120 MHz. It is believed, on the basis of measurements made during the development of the breadboard system, that the deflection frequency could have been raised to 180 MHz, with adequately large voltage, without major changes in the apparatus. The principal limiting factors are the interelectrode capacitances and conductor inductances inside the image converter tube. It seems reasonable to expect that, with special attention to these capacitances and inductances, a tube could be built to operate at still higher frequencies.

The work of Bradley, et al. (Ref. 2) and Schelev, et al. (Ref. 3) indicates that the ultimate timing resolution achievable by the image converter technique should be 5 psec or less. As was mentioned in the Introduction, this sort of timing accuracy would make it possible to use the

two-color method to reduce the uncertainty in the atmospheric correction, independently of any measurements of atmospheric parameters. If the two wavelengths used were $\lambda 694$ μm and $\lambda 347$ μm (the ruby laser wavelength and the wavelength obtained by frequency-doubling the ruby output), the error in the atmospheric correction derived from the two range measurements would be about 10 times as great as that associated with the range measurements themselves. Thus a time-of-flight measurement to 5 psec (corresponding to a one-way range uncertainty of .075 cm) would yield a value for the atmospheric correction good to better than 1 cm, a useful, if not startling, improvement.

As was also noted in the Introduction, the full potential of the new vernier system cannot be realized until better satellite retroreflectors are in orbit. The same basic technique, however, can be used in a different way to improve the accuracy of laser ranging to existing satellites, with their retroreflectors consisting of arrays of small corner cubes. When the transition to mode-locked laser transmitters has been completed, the ranging pulse is likely to be less than 100 psec in duration. The return pulse, however, will be made up of contributions reflected from different elements of the reflector array and may therefore be several nanoseconds long. In an image converter system like that of the vernier discussed in this report a one-to-one correspondence could be established between the duration and temporal variation of the return laser pulse and the length and intensity variation of the image on the phosphor screen. An appropriate read-out system could then provide a digitized output representing the wave-form (intensity versus time) of the reflected laser pulse. From these data, coupled with information about the geometrical configuration of the spacecraft and retroreflector, it should be possible to determine the attitude of the satellite and to extract the range of the center of mass of the satellite (rather than simply the range of the center of the reflector array). Furthermore,

examination of such wave-form data should permit the development of better ways of determining the (temporal) location of the centroid of the return pulse or, perhaps, of some other fiducial time within the pulse. Any such improvement would reduce the uncertainty of the basic range measurement.

VII. APPENDIX

In this appendix are gathered three items of detail: a parts list for the image converter chassis (Table A1), a detailed schematic diagram of the image converter chassis (Fig. A1), and a schematic of the voltage distribution system for the image converter chassis (Fig. A2).

TABLE A1

Parts List for Image Converter Chassis

C_1	E. F. JOHNSON 193-0010-001, 2.2 TO 34 pF, INPUT LOOP TUNING
C_2	E. F. JOHNSON 160-0303-001, 1.5 TO 5.0 pF, GRID BAL. ADJ.
C_3	PISTON TRIMMER, VC43GW, 0.8 TO 30 pF
C_4	HAMMERLUND HFD25, 25pF/SECTION, GRID CKT. TUNING
C_5, C_6	SCREEN BYPASS, PART OF EIMAC 620A TUBE SOCKET
C_7, C_8	NEUTRALIZING TABS
C_9, C_{10}, C_{11}	SPRAGUE 709C2, 500 pF, 30KVDC
C_{12}	SPRAGUE 708C50, 500 pF, 20KVDC
L_1	1/4 in. × 5-1/2 in. COPPER STRIP
L_2	3/16 in. COPPER TUBING
L_3	0.090 in. BRASS STRIPS
RFC 1, RFC 2	48 TURNS No. 24 ENAMEL SPACE WOUND ON 5/8 in. × 2-1/4 in. FIBERGLASS ROD
RFC 3	32 TURNS No. 24 ENAMEL CLOSEWOUND ON 1/4 in. TEFLON ROD
V_1, V_2	EIMAC 4C X 250B

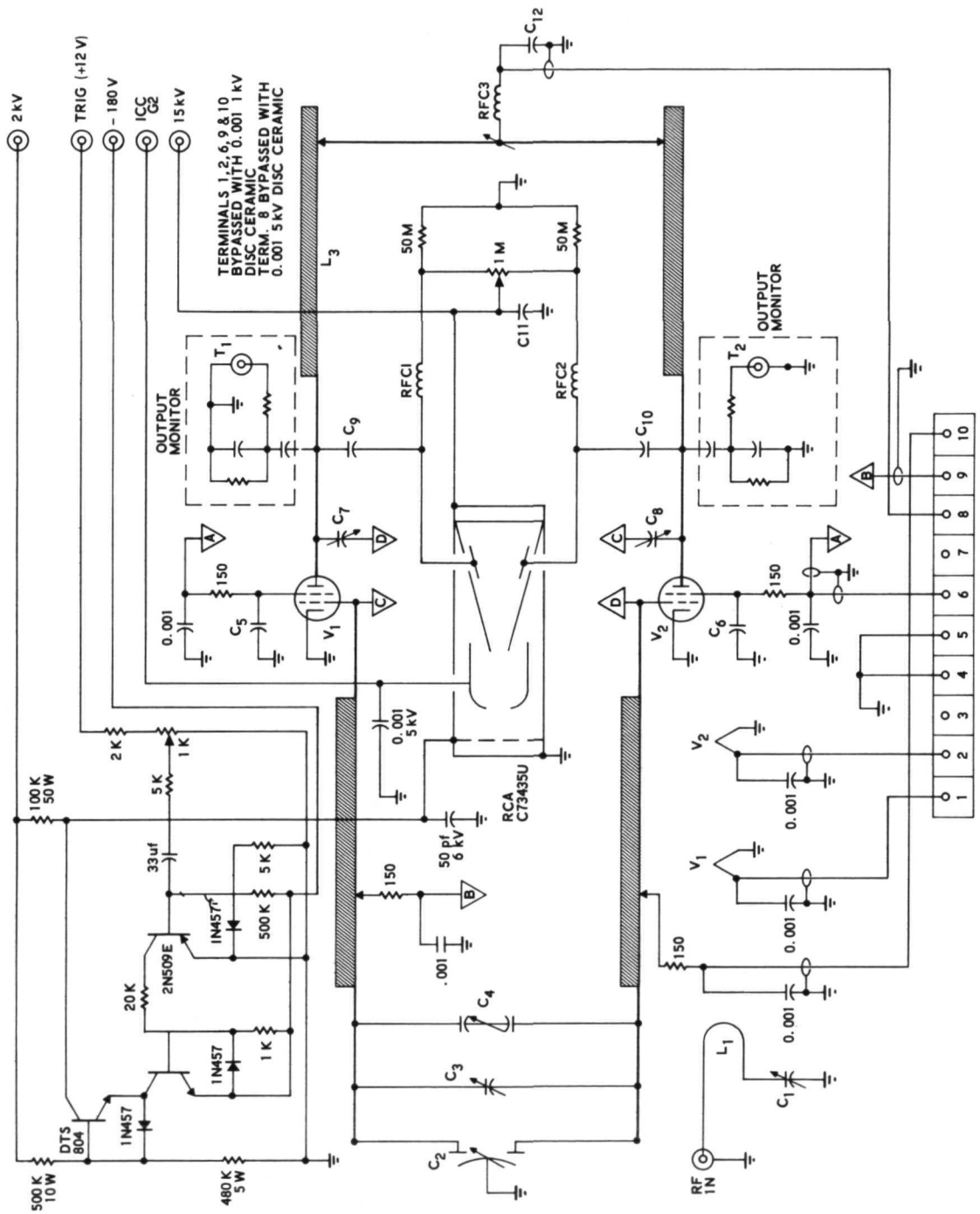

Fig. A1. Detailed Schematic of Image Converter Chassis

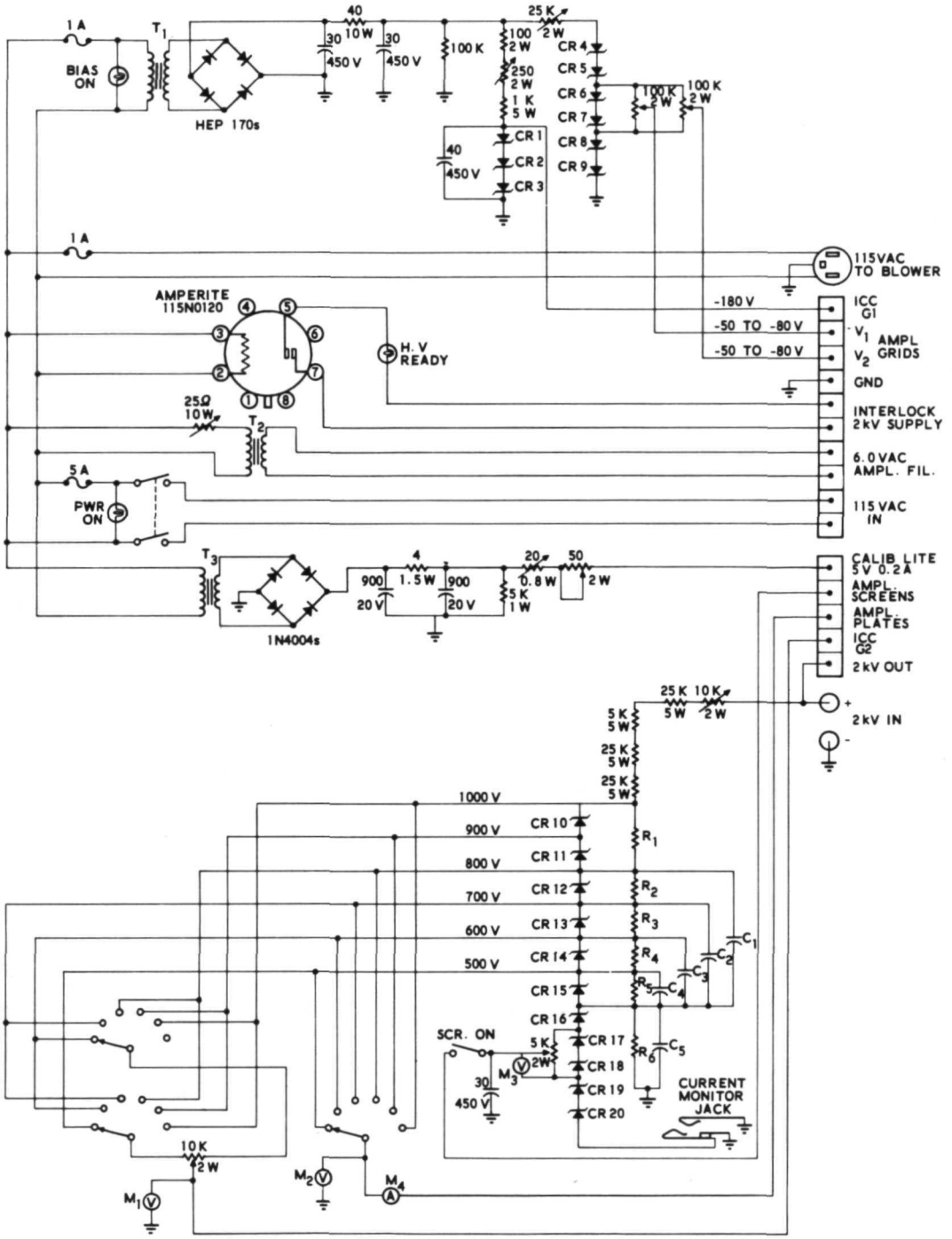

Fig. A2. Schematic of Voltage Distribution System for Image Converter Chassis

VIII. REFERENCES

1. Massachusetts Institute of Technology: The Terrestrial Environment: Solid-Earth and Ocean Physics. NASA CR-1579, 1970.

2. Bradley, D. J.; Liddy, B.; and Sleat, W. E.: Direct Linear Measurement of Ultrashort Light Pulses with a Picosecond Streak Camera. Opt. Commun., vol. 2, no. 8, Jan. 1971, pp. 391-395.

3. Schelev, M. Ya.; Richardson, M. C.; and Alcock, A. J.: Image Converter Streak Camera with Picosecond Resolution. Appl. Phys. Lett., vol. 18, no. 8, Apr. 15, 1971, pp. 354-357.

4. Fowler, R. A.: Earthquake Prediction from Laser Surveying. NASA SP-5042, 1968.

5. DeMaria, A. J.; Glenn, W. H. Jr.; Brienza, M. J.; and Mack, M. E.: Picosecond Laser Pulses. Proc. IEEE, vol. 57, no. 1, Jan. 1969, pp. 2-25.

6. Boyle, W. S.; and Smith, G. E.: Charge-coupled Devices — A New Approach to MIS Device Structures. IEEE Spectrum, vol. 8, no. 7, July 1971, pp. 18-27.

☆ U. S. GOVERNMENT PRINTING OFFICE: 1973—736-652/16 REGION NO. 3-II.

NATIONAL AERONAUTICS AND SPACE ADMINISTRATION
WASHINGTON, D.C. 20546

OFFICIAL BUSINESS
PENALTY FOR PRIVATE USE $300

SPECIAL FOURTH-CLASS RATE BOOK

POSTAGE AND FEES PAID
NATIONAL AERONAUTICS AND SPACE ADMINISTRATION
451

U.S.MAIL

POSTMASTER: If Undeliverable (Section 158 Postal Manual) Do Not Return

"The aeronautical and space activities of the United States shall be conducted so as to contribute . . . to the expansion of human knowledge of phenomena in the atmosphere and space. The Administration shall provide for the widest practicable and appropriate dissemination of information concerning its activities and the results thereof."

—NATIONAL AERONAUTICS AND SPACE ACT OF 1958

NASA SCIENTIFIC AND TECHNICAL PUBLICATIONS

TECHNICAL REPORTS: Scientific and technical information considered important, complete, and a lasting contribution to existing knowledge.

TECHNICAL NOTES: Information less broad in scope but nevertheless of importance as a contribution to existing knowledge.

TECHNICAL MEMORANDUMS: Information receiving limited distribution because of preliminary data, security classification, or other reasons. Also includes conference proceedings with either limited or unlimited distribution.

CONTRACTOR REPORTS: Scientific and technical information generated under a NASA contract or grant and considered an important contribution to existing knowledge.

TECHNICAL TRANSLATIONS: Information published in a foreign language considered to merit NASA distribution in English.

SPECIAL PUBLICATIONS: Information derived from or of value to NASA activities. Publications include final reports of major projects, monographs, data compilations, handbooks, sourcebooks, and special bibliographies.

TECHNOLOGY UTILIZATION PUBLICATIONS: Information on technology used by NASA that may be of particular interest in commercial and other non-aerospace applications. Publications include Tech Briefs, Technology Utilization Reports and Technology Surveys.

Details on the availability of these publications may be obtained from:

SCIENTIFIC AND TECHNICAL INFORMATION OFFICE

NATIONAL AERONAUTICS AND SPACE ADMINISTRATION

Washington, D.C. 20546